THE JOURNAL OF BIOLOGICAL CHEMISTRY VOL. 284, NO. 2, pp. 1252–1266, January 9, 2009

N-Methyl-D-aspartate Receptor Subunits Are Non-myosin Targets of Myosin Regulatory Light Chain*

Received for publication, March 7, 2008, and in revised form, October 7, 2008 Published, JBC Papers in Press, October 21, 2008, DOI 10.1074/jbc.M801861200

Gaurav Bajaj[‡], Yong Zhang[‡], Michael I. Schimerlik[§], Andrew M. Hau[‡], Jing Yang[‡], Theresa M. Filtz[‡], Chrissa Kioussi[‡], and Jane E. Ishmael[‡1]

From the [‡]Department of Pharmaceutical Sciences, College of Pharmacy, and the [§]Department of Biochemistry and Biophysics, Oregon State University, Corvallis, Oregon 97331

Excitatory synapses contain multiple members of the myosin superfamily of molecular motors for which functions have not been assigned. In this study we characterized the molecular determinants of myosin regulatory light chain (RLC) binding to two major subunits of the *N*-methyl-D-aspartate receptor (NR). Myosin RLC bound to NR subunits in a manner that could be distinguished from the interaction of RLC with the neck region of non-muscle myosin II-B (NMII-B) heavy chain; NR-RLC interactions did not require the addition of magnesium, were maintained in the absence of the fourth EF-hand domain of the light chain, and were sensitive to RLC phosphorylation. Equilibrium fluorescence spectroscopy experiments indicate that the affinity of myosin RLC for NR1 is high (30 nM) in the context of the isolated light chain. Binding was not favored in the context of a recombinant NMII-B subfragment one, indicating that if the RLC is already bound to NMII-B it is unlikely to form a bridge between two binding partners. We report that sequence similarity in the "G*XXX*R" portion of the incomplete IQ2 motif found in NMII heavy chain isoforms likely contributes to recognition of NR2A as a non-myosin target of the RLC. Using site-directed mutagenesis to disrupt NR2A-RLC binding in intact cells, we find that RLC interactions facilitate trafficking of NR1/NR2A receptors to the cell membrane. We suggest that myosin RLC can adopt target-dependent conformations and that a role for this light chain in protein trafficking may be independent of the myosin II complex.

Regulation and maintenance of glutamate receptor numbers at postsynaptic sites are critical for excitatory neurotransmission in the central nervous system. Mechanisms that underlie targeting of glutamate receptors to synapses almost certainly involve a regulated series of protein-protein interactions between the receptor and various binding partners. In trying to understand how these events are temporally and spatially coordinated, the intracellular carboxyl termini of glutamate receptor subunits have attracted much attention as they have been shown to bind directly and indirectly to a number of cytoskeletal and motor proteins, scaffolding proteins, enzymes, and other signaling molecules (1). We have previously demonstrated that three major subunits of the *N*-methyl-D-aspartate (NMDA)[2] subtype of ionotropic glutamate receptor bind directly to myosin II regulatory light chain (RLC) (2). Myosin RLC is an accessory light chain of the actin-based motor myosin II, which is a hexameric complex composed of two heavy chains, two RLCs, and two essential light chains (ELC) (3). Myosin II light chains are, like calmodulin, members of the EF-hand family of calcium-binding proteins (4). However, the interaction of myosin RLC with NMDA receptor (NR) subunits could be distinguished from the strictly Ca^{2+}-dependent interaction of calmodulin with the NR1 subunit (2).

The light chains of myosin II are integral components of the myosin II complex that bind to tandem IQ motifs located in the neck region of myosin II heavy chain. An IQ motif is approximately 25 amino acids long containing the classic consensus sequence IQ*XXX*RG*XXX*R (5). Variations in this consensus IQ sequence can, however, explain both the light chain binding preference of heavy chains and also the particular conformation that a light chain can adopt upon binding (6–8). For example, RLCs of myosin II are predicted to adopt an extended conformation when bound to the neck region of myosin II heavy chain (9, 10). However, crystallographic evidence indicates the ELC of *Saccharomyces cerevisiae*, Mlc1p, can exist in the following two distinct conformations: compact and extended depending on the specific IQ sequence of the myosin heavy chain (8). When bound in an extended conformation, it is suggested that Mlc1p has a free amino terminus that may interact with another binding partner to form a ternary complex with myosin II heavy chain (8). This finding has attracted much attention because ELC in organisms such as *S. cerevisiae*, *Schizosaccharomyces pombe*, and *Drosophila melanogaster* have several binding partners (11). These include class II myosin heavy chains (Myo1p in *S. cerevisiae* (12, 13), Myp2 and Myo2 in *S. pombe* (14), and *zipper* in *D. melanogaster* (11)), myosin V heavy chains (11, 15), additional unconventional myosins (VI and VIIa in *D. melanogaster* (11)), cytoskeletal IQ containing

* This work was supported, in part, by National Institutes of Health Grants R01AR054406 and P30-ES000210. This work was also supported by American Heart Association Award 0060435Z, P30-ES000210. The costs of publication of this article were defrayed in part by the payment of page charges. This article must therefore be hereby marked "*advertisement*" in accordance with 18 U.S.C. Section 1734 solely to indicate this fact.

[1] To whom correspondence should be addressed. Tel.: 541-737-5783; Fax: 541-737-3999; E-mail: jane.ishmael@oregonstate.edu.

[2] The abbreviations used are: NMDA, *N*-methyl-D-aspartate; NR, NMDA receptor; RLC, regulatory light chain; NMII-B, non-muscle myosin II-B; NMIIB S1, SMIIB subfragment 1; GST, glutathione *S*-transferase; ELC, essential light chain; BSEP, bile salt export protein; ABC, ATP-binding cassette; MHC, myosin II-B heavy chain; MLC, myosin light chain; MLCK, MLC kinase; HEK, human embryonic kidney; CFP, cyan fluorescent protein; YFP, yellow fluorescent protein; DTT, dithiothreitol; MRLC, myosin RLC; DL-AP5, DL-2-amino-5-phosphonopentanoic acid.

GTPase-activating protein-like proteins (16–18), and a microtubule-associated protein (11).

Myosin RLC has also been reported to interact with a number of proteins other than myosin II heavy chain. In addition to NMDA-type glutamate receptor subunits (2), myosin RLC binds via its amino terminus to the smooth muscle protein calponin (19). The RLC also binds directly to bile salt export protein (BSEP) and at least two other members of the family of ATP-binding cassette (ABC) family of drug efflux transporters (20), as well as a novel ezrin, radixin, moesin (ERM)-like protein, with ubiquitin-protein isopeptide ligase activity, known as myosin regulatory light chain-interacting protein (MIR in human brain (21–24) and Mir in zebrafish (25, 26)). As it is widely assumed that RLC functions only in the context of a myosin II complex, the existence of these additional binding partners raises the possibility that the RLC could form a ternary complex with myosin II heavy chain and a third non-myosin binding partner (20, 24). The goals of this study were as follows: 1) to determine whether brain myosin RLC can bind to two target sequences simultaneously, and 2) to determine the physiological relevance of RLC-NMDA receptor interactions. We report that RLC binds NR1 and NR2 subunits in a manner that can be clearly distinguished from the interaction of RLC with the neck region of non-muscle myosin II heavy chain. Equilibrium fluorescence spectroscopy experiments revealed that the affinity of myosin RLC for NR1 is high in the context of the isolated light chain, but is not favored if the RLC was already in a complex with myosin II heavy chain. By focusing on the membrane-proximal region of the NR2A subunit, which is not a target of calmodulin, we report that sequence homology in the "G*XXX*R" portion of the incomplete IQ2 motif found in all three non-muscle myosin II heavy chain isoforms likely contributes to the recognition of NR2 subunits as a non-myosin target of the RLC. Using site-directed mutagenesis to disrupt myosin RLC binding in intact cells, we find that RLC interactions likely occur within the Golgi secretory trafficking pathway. Disruption of RLC binding to NR2A resulted in a delay in delivery of functional NR1/ΔNR2A receptors to the cell membrane. Our data suggest a role for myosin RLC that is independent of the typical interaction of the light chain with myosin II heavy chain.

EXPERIMENTAL PROCEDURES

Plasmids and Constructs—Plasmids containing rat NMDAR2A, NMDAR2B, and NMDAR1-1a cDNAs have been described previously (2). The human MHC-B clone HB5.12/1.21, used to construct MHC-(771–843) encoding the neck region of non-muscle myosin II-B (MHC-B) in pGEX-2T (2), was a kind gift from Dr. R. Adelstein (National Institutes of Health, Bethesda). The membrane-proximal region of the carboxyl terminus of the NMDAR2A subunit (amino acid residues 838–874) in pGEX-6P-3 was the generous gift of Dr. J. Saugstad (Robert S. Dow Neurobiology Laboratories, Portland, OR).

For bacterial expression, NR2A-(875–1029), NR2A-(1030–1464), NR2A-(1030–1290), NR2A-(1291–1464), NR2A-(838–867) (known as Δ868), NR2A-(838–860) (known as Δ861), and NR2A-(838–854) (known as Δ855) were amplified by PCR and inserted into the bacterial expression vector pGEX-6P-3 (GE Healthcare). The membrane-proximal region of the carboxyl terminus of the NMDAR2B subunit (amino acid residues 839–873) was amplified by PCR and inserted into pGEX-6P-3. Myosin regulatory light chain-(1–101), RLC-(102–172), RLC-(1–129), RLC-(61–129), and RLC-(61–172) were amplified by PCR from the mouse pACT2/5-6-1 clone (2) and inserted into the bacterial expression vector pET 28a (Novagen, Madison, WI). The construction of full-length myosin RLC-(1–172), NMDAR1-(834–938), NR1-(834–863) (encoding C0), NR1-(864–938) (encoding C1C2), and NR1-(834–855) (known as Δ856) has been described previously (2). For expression in mammalian cells, NR2A-(1–1028) and RLC-(1–172) were amplified by PCR and inserted into EcoRI and XhoI sites of pECFP-N1 and pEYFP-N1 (Clontech), respectively. NR1 was excised from the plasmid pTL1/NR1-1a (27) and inserted into HindIII and XbaI restriction sites of pCDNA 3.1 (Invitrogen). Full-length RLC-(1–172) was also inserted into pCDNA 3.1. Site-directed mutagenesis was performed using standard techniques. All sequences were confirmed by the Center for Genome Research and Biocomputing Core Facility (Oregon State University, Corvallis, OR).

Antibodies—The anti-myosin RLC antibody (αMRLC/3) was raised in rabbits against a unique peptide and has been described previously (2). Antiserum to the phosphorylated form of serine 19 of myosin RLC was also raised in rabbits against a unique phosphopeptide (CRPQRATS-PO3-NVFAM) and affinity-purified (αMRLC/P) (Bethyl Laboratories Inc., Montgomery, TX). The anti-GST antibody was a gift of Dr. Mark Leid (Oregon State University, Corvallis, OR). Other primary antibodies used in this study are commercially available and included the following: anti-calmodulin (Upstate Biotechnology Inc., Lake Placid, NY), anti-PSD95 (Affinity Bioreagents Inc., Golden, CO), anti-myosin light chain (MLC) (Abcam, Cambridge, MA), anti-T7 (Novagen, Madison, WI), anti-adaptin α (Transduction Laboratories, Newington, NH), anti-Golgi 58K protein (clone 58K-9) and anti-FLAG (both from Sigma), and anti-non-muscle myosin heavy chain isoforms IIA and IIB (both from Covance Research Products, Denver, PA).

Protein Purification—Recombinant myosin RLC was expressed in *Escherichia coli* (BL21-Gold(DE3)pLysS; Stratagene, La Jolla, CA) and purified by nickel-chelate chromatography. The polyhistidine tag was removed by thrombin cleavage (Thrombin Clean Cleave kit; Sigma) followed by dialysis against a buffer containing 20 mM Tris (pH 7.7) and 500 mM NaCl. GST fusion proteins were bacterially expressed, as above, and purified by column chromatography using immobilized glutathione (Pierce). The bound GST fusion protein was eluted using a buffer containing 10 mM reduced glutathione and 50 mM Tris-HCl (pH 8.0) followed by dialysis against the buffer containing 50 mM Tris-HCl (pH 8.0). Native smooth muscle myosin light chain (MLC-2) was isolated and purified from washed turkey gizzard myofibrils as described previously (28, 29), and was a kind gift from Drs. Sonia Anderson and Dean Malencik (Oregon State University, Corvallis, OR). Smooth muscle myosin light chain kinase (MLCK) was a kind gift from Dr. Christine Cremo (University of Reno, NV). Bovine calmodulin was purchased from Calbiochem. Purified FLAG-tagged human non-muscle IIB subfragment 1 (NMIIB S1), a truncated

myosin heavy chain fragment co-expressed with regulatory and essential myosin light chains in baculovirus (30), was a kind gift of Dr. James Sellers (National Institutes of Health, Bethesda).

Phosphorylation of Isolated RLC and NMIIB S1—Regulatory light chain RLC, either in isolated form or in the context of NMIIB S1, was phosphorylated in the presence of smooth muscle MLCK (31). Isolated RLC or NMIIB S1 was added to a buffer containing 20 mM Tris (pH 7.5), 0.1 mM EGTA, 1 mM DTT, 10 μg/ml MLCK, 10 μg/ml calmodulin, 5 mM $MgCl_2$, 1.5 mM $CaCl_2$, and 1 mM ATP and incubated at 37 °C for 1 h. Phosphorylation of each sample was verified by PAGE in the presence of urea; control samples were nonphosphorylated or subjected to mock phosphorylation reactions (lacking MLCK). Samples were heated at 80 °C for 2 min in urea sample buffer (8 M urea, 33 mM Tris-glycine (pH 8.6), 0,17 mM EDTA, and bromphenol blue), before loading on NOVEX Tris-glycine pre-cast gels (Invitrogen). Proteins were visualized directly by Coomassie Blue stain (Bio-Rad) or were electrotransferred to nitrocellulose membrane (Amersham Biosciences) and detected by immunoblot with either a T7 tag antibody (RLC), αMRLC/P (phosphorylated RLC), anti-FLAG antibody (heavy chain), or anti-MLC1 (ELC) and appropriate horseradish peroxidase-conjugated secondary antibodies (Calbiochem). Immune complexes were revealed using a chemiluminescence assay (Roche Diagnostics).

Fluorescence Spectroscopy—A peptide corresponding to the first 30 amino acids of the carboxyl tail of the NMDAR1 subunit (residues 834–863) was labeled with fluorescein on the amino terminus (FITC-EIAYKRHKDARRKQMQLAFAAVNVWRK-NLQ-COOH) and purified by reverse phase high pressure liquid chromatography (United Biochemical Research, Inc., Seattle, WA). Fluorescence measurements were taken in 2.0 ml of buffer containing 20 mM Tris (pH 7.7), 500 mM NaCl and a final peptide concentration of 300 nM. Purified RLC was added from a concentrated stock solution and allowed to equilibrate in the dark for 5 min prior to fluorescence determinations. All additions of purified RLC were made sequentially from a single stock solution, and the fluorescence emission was corrected for dilution. All experiments were performed on an SLM 8000C spectrofluorometer (SLM Instruments, Urbana, IL). Data were fit to Equation 1 by weighted nonlinear least squares using the computer program Scientist® (Micromath Inc., St. Louis, MO) when the weighting factors were equal to the square of the reciprocal of the standard deviation for each data point,

$$F = a + b\left\{\frac{2R_0L_0}{R_0 + L_0 + K + \sqrt{(R_0 + L_0 + K)^2 - 4R_0L_0}}\right\} + cL_0 \quad \text{(Eq. 1)}$$

where F is the measured fluorescence enhancement; a is the fluorescence observed in the absence of RLC; R_0 is the total concentration of fluorescently labeled peptide; L_0 is the total concentration of RLC; K is the dissociation constant for the peptide-protein complex; b is the relative fluorescence enhancement of the fluorescent peptide-protein complex; and c is a parameter used to fit the background linear fluorescence increase observed as the RLC concentration increased.

Fluorescence Microscopy, Culture, and Transfection of Mammalian Cells—Human embryonic kidney cells (HEK) 293 cells were maintained in 90% Dulbecco's modified Eagle's medium (Mediatech, Herndon, VA), 10% fetal bovine serum (HyClone, Logan, UT), 100 units/ml penicillin, and 0.1 mg/ml streptomycin at 37 °C under 5% CO_2 in humidified air. The day before transfection, cells (2×10^4) were plated on poly-L-lysine-coated glass coverslips in medium supplemented with kynurenic acid (3 mM, Sigma) and DL-AP5 (1 mM Tocris, Ellisville, MO) (32). Cells were transfected using FuGENE 6 (Roche Diagnostics) and maintained for up to 72 h. Cells were then washed twice with 1× phosphate-buffered saline, fixed in 3% formaldehyde (20 min), and mounted on slides with a ProLong® antifade kit (Molecular Probes, Eugene, OR). Confocal images were obtained using a Zeiss LSM510 confocal microscope (Carl Zeiss, Thornwood, NY) with a Zeiss 63× oil immersion objective. Fluorescence signals were collected using laser excitation at 514 nm for YFP and 458 nm for CFP. LP 530 and BP 470–500 filters were used for detection of YFP and CFP emission as described previously (33). For detection of endogenous K58 Golgi protein and heavy chain isoforms, sections were incubated with appropriate primary antibodies after fixation followed by secondary antibodies conjugated to Alexa 546 or Cy5, respectively.

Glutathione S-Transferase (GST) Pulldown Assays—Pulldown assays from brain homogenates (extracted in a buffer containing 250 mM NaCl and 10 mM ATP) were conducted as described previously (2). Pulldown assays with recombinant myosin RLC and the carboxyl regions of NR1 or the NMII-B heavy chain neck region have also been described (2) but included the following modifications: 1) assays were initiated with the addition of recombinant RLC (100 nM), and 2) the incubation time was extended to 2 h. For studies to determine the interaction of full-length and mutant RLC (phosphorylated and nonphosphorylated) with the NR2A subunit, GST fusion proteins or GST alone was incubated in binding buffer (10 mM HEPES (pH 7.5), 100 mM NaCl, 1 mM EDTA, 1 mM dithiothreitol (DTT), 0.1% Nonidet P-40 and 10% glycerol) and allowed to proceed for 2 h at 4 °C as described above. Unbound protein was removed by three sequential washes with binding buffer, and bound proteins were eluted from the beads by boiling in sample buffer. Proteins were separated by SDS-PAGE, transferred to nitrocellulose membranes, and processed for immunoblot analysis as described above. Calcium-dependent calmodulin binding to NMDA receptor subunits was assessed in the same way in the absence (binding buffer) or presence of calcium (binding buffer lacking EDTA but including 2 mM calcium chloride). The magnesium dependence of RLC binding was also assessed in the absence and presence of magnesium (lacking EDTA but including 1 mM magnesium chloride). In all calcium and magnesium studies, the appropriate binding buffer was used in all subsequent washes to remove unbound protein. In light of the apparent magnesium dependence of RLC binding to the neck region of NMII-B heavy chain, subsequent studies were carried out in the presence of magnesium (1 mM).

Immunopreciptation Studies—NR2A-(838–874) fused to GST (150 nM) was purified and mixed with either purified NMIIB S1, NMIIB S1-P, or bacterially expressed myosin RLC

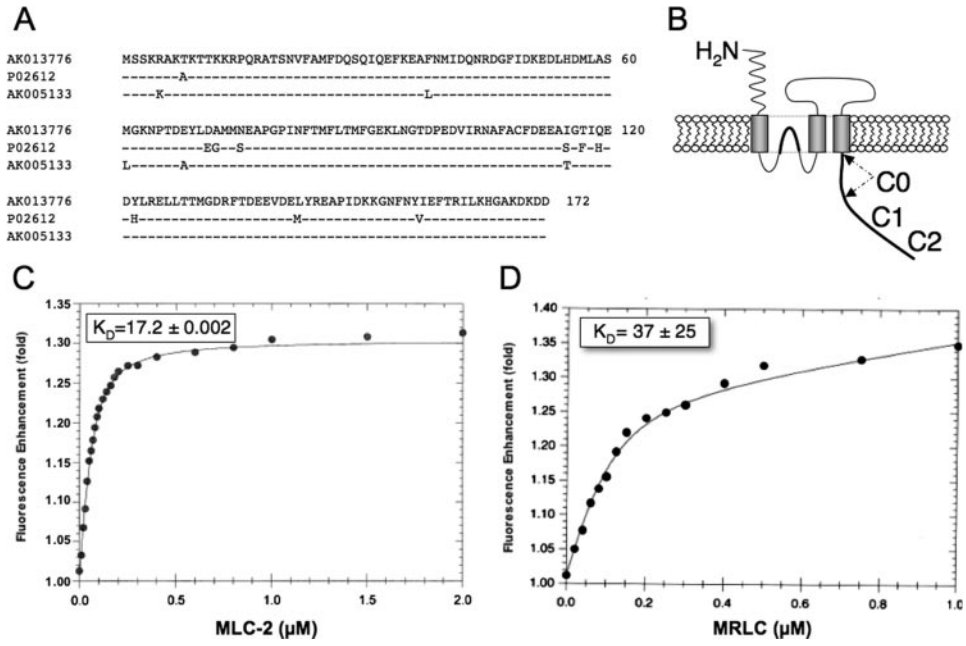

FIGURE 1. **Myosin RLC isoforms enhance fluorescence emission of a fluorescein-labeled peptide corresponding to the C0 region of the NMDAR1 carboxyl tail.** *A,* amino acid sequence of a myosin RLC isoform previously identified in mouse hippocampus (GenBank™ accession number AK013776), the major smooth muscle RLC isoform in chicken gizzard (GenBank™ accession number P02612), and an RLC isoform identified from mouse cerebellum (GenBank™ accession number AK005133). AK013776 is identical to the isoform previously identified in mouse brain (MRLC) as an NMDA-receptor interacting protein (2). *B,* schematic representation of the NMDAR1 subunit showing the location of C0, C1, and C2 regions. *C* and *D,* titration of either purified smooth muscle MLC-2 (*C*) or purified, recombinant MRLC (*D*) enhanced fluorescence emission by ~30%. Data were fit to a single hyperbolic curve using Equation 1 to derive binding affinities of 37 ± 25 nM (a = 1.0110 ± 0.0001, b = 2.6 ± 0.9, c = 0.09 ± 0.03, R_0 = 0.10 ± 0.03, and r^2 = 0.999) for MRLC (*C*), and 17.2 ± 2.2 nM (a = 0.996 ± 0.004, b = 7.42 ± 0.54, c = 0.029 ± 0.006, R_0 = 0.073 ± 0.004, and r^2 = 0.999) for MLC-2 (*D*). Each point represents fluorescence determined in quadruplicate; standard errors lie within the data points.

(MRLC) in 10 mM HEPES containing 0.1% Nonidet P-40, 100 mM NaCl, 1 mM EDTA, 1 mM DTT, 10% glycerol (pH 7.5) at 4 °C. Bovine serum albumin was added to a final concentration of 0.5%, and proteins were allowed to incubate with gentle rotation for 2 h at 4 °C. Anti-GST (12 μg) was then added to the samples and allowed to incubate with gentle rotation for a further 2 h at 4 °C. Precipitation of immune complexes was facilitated by the addition of a 25-μl aliquot of 50% protein G-Sepharose slurry (Amersham Biosciences) to each tube, incubated with gentle rotation for 2 h at 4 °C. Immune complexes were collected by centrifugation at 3,000 × *g* for 1 min, followed by three consecutive resuspension/wash and centrifugation steps. Precipitated proteins were eluted from the beads by heating for 2 min in 2× Laemmli sample buffer. Proteins were separated by SDS-PAGE, transferred to nitrocellulose membranes, and processed for immunoblot analysis as described above.

RESULTS

Smooth Muscle and Brain Isoforms of Myosin RLC Bind to the NR1 Subunit with High Affinity—Although there is considerable sequence homology at the amino acid level among RLCs in non-muscle and smooth muscle tissues, subtle differences have been noted between brain isoforms (34–36) and the well characterized smooth muscle isoform of RLC (37) (Fig. 1*A*). To determine whether these small differences in amino acid sequence were sufficient to influence binding of myosin RLC to the NMDA receptor, we determined binding affinities for the mouse brain isoform, previously identified as an NMDA receptor-interacting protein (GenBank™ accession number AK013776), and the major smooth muscle isoform from chicken gizzard (GenBank™ accession number P02612) using equilibrium fluorescence spectroscopy. These initial binding studies were conducted at supra-physiological salt concentrations (0.5 M NaCl), to distinguish RLC-NR1 interactions from those, such as calponin (19), that may be strictly limited to low ionic strength conditions. Functional NMDA receptors differ with respect to their complement of NR2 subunits, but the first 30-amino acid region of the carboxyl terminus of NR1 (referred to as C0; Fig. 1*B*) is conserved in all splice variants of NR1 and thus present in all functional NMDA receptors. As we have previously determined that NR1-C0 is necessary and sufficient for myosin RLC binding (2), we used a fluorescein-labeled peptide (F-NR1-C0) corresponding to this entire region for our fluorescence binding studies. The F-NR1-C0 peptide alone exhibited maximum excitation at 493 nm and maximum emission at 520 nm (data not shown). Titration of either smooth muscle light chain, isolated and purified from chicken gizzard (Fig. 1*C*), or purified, recombinant brain (Fig. 1*D*) enhanced the fluorescence emission of F-NR1-C0 by ~30%. These data were best fit by a single hyperbolic curve using a nonlinear, curve fitting analysis, allowing us to derive binding affinities of 37 ± 24 and 17 ± 2.2 nM for brain and chicken gizzard RLC isoforms (Fig. 1, *C* and *D*), respectively. The affinity of chicken gizzard RLC for F-NR1-C0 was not significantly different when the buffer containing half-molar salt was substituted for phosphate-buffered saline (29 nM; data not shown). Given the large degree of sequence homology between brain and smooth muscle isoforms and the fact that both bind to the C0 region of NR1 with comparable affinity, it appears unlikely that myosin RLC-NMDA receptor interactions can be explained by unique characteristics of RLC isoforms present in rodent brain.

Light Chain-NMDA Receptor Interactions Are Not Dependent upon Magnesium—As Mg^{2+} is thought to fulfill a key structural requirement for RLC binding to myosin II heavy chain, we compared the magnesium dependence of NR1 and heavy chain interactions. For these studies, the full-length carboxyl terminus of NR1 fused to GST and the neck region of non-muscle myosin II-B heavy chain fused to GST were expressed in bacteria and examined for interaction with RLC in the presence and absence of Mg^{2+} (Fig. 2). Although Mg^{2+} enhanced binding of myosin RLC to both interaction partners, RLC-NR1 interac-

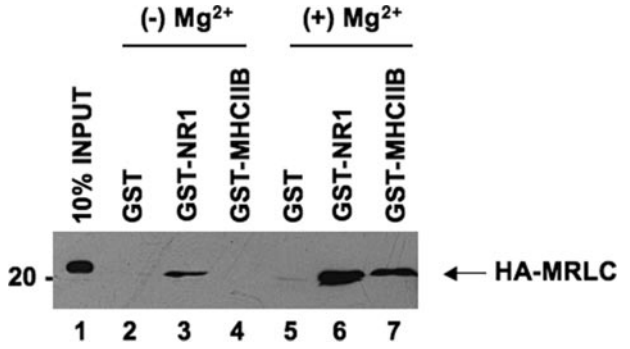

FIGURE 2. **Light chain binding to NMDA receptor subunits does not require added magnesium.** A direct comparison of light chain binding to the carboxyl terminus of NR1 and the neck region myosin IIB heavy chain revealed that NR1-RLC interactions are less sensitive to the effects of Mg^{2+}. The carboxyl tail of NR1-(834–938) and the neck region of non-muscle myosin heavy chain IIB-(771–843), each fused to GST, were immobilized on glutathione-Sepharose beads for use in GST pulldown experiments. GST fusion proteins or GST alone were used as affinity matrices to examine interactions with purified, recombinant myosin RLC in the absence (*lanes 2–4*) or presence (*lanes 5–7*) of 1 mM Mg^{2+}. Assays were initiated by the addition of 300 nM myosin RLC and incubated with rotation for 2 h at 4 °C. Immune complexes were revealed using an anti-T-7 antibody (Novagen) to detect recombinant myosin RLC. Figure is representative of three independent experiments.

tions appeared to be much less dependent upon Mg^{2+} (Fig. 2). Consistent with our previous studies (2), myosin RLC showed a specific interaction with the NR1 carboxyl terminus in the absence of added Mg^{2+} (Fig. 2, *lane 3*), whereas no interaction was detected between myosin II heavy chain and RLC under the same conditions (Fig. 2, *lane 4*). These findings suggest that RLC-NMDA receptor complexes may be distinguished from RLC-myosin II heavy chain complexes *in vitro* on the basis of their sensitivity to Mg^{2+}. As our peptide binding studies, carried out in the absence of added Mg^{2+}, revealed no major distinction between RLC isoforms, the basis for this difference likely resides within the target sequence itself. Taken together, these observations support a role for NMDA receptor subunits as non-myosin targets of the RLC.

Myosin RLC Interacts with the Intracellular Membrane-proximal Region of the Carboxyl Terminus of NR2 Subunits—We have previously shown that myosin RLC binds directly to the carboxyl-terminal region NR1 and NR2 subunits (2). However, the carboxyl termini of NR2 family subunits are roughly six times longer than those of the NR1 subunit (~600 amino acids *versus* 90 amino acids). We used a series of deletion mutants (Fig. 3*A*) to map regions of the NR2A cytoplasmic tail required for interaction with myosin RLC. Truncation mutants were expressed in bacteria as GST fusion proteins and immobilized on glutathione-Sepharose beads. Immobilized GST/NMDA receptor fusion proteins and GST alone were then used as affinity matrices to examine interactions with RLC from homogenates derived from mouse forebrain (*lower panel* of Fig. 3*B*). Immunoblotting with an anti-myosin RLC antibody revealed that native mouse brain RLC interacted strongly and specifically with GST/NR2A-(838–874) corresponding to the first 37 amino acids of the NR2A carboxyl terminus (Fig. 3*B, lane 5*) but failed to interact with GST/NR2A-(875–1029), GST/NR2A-(1030–1464), and GST/NR2A-(1030–1290) (Fig. 3*B, lanes 6–8*). A faint immunoreactive signal was observed corresponding to retention of native myosin RLC on a GST affinity matrix

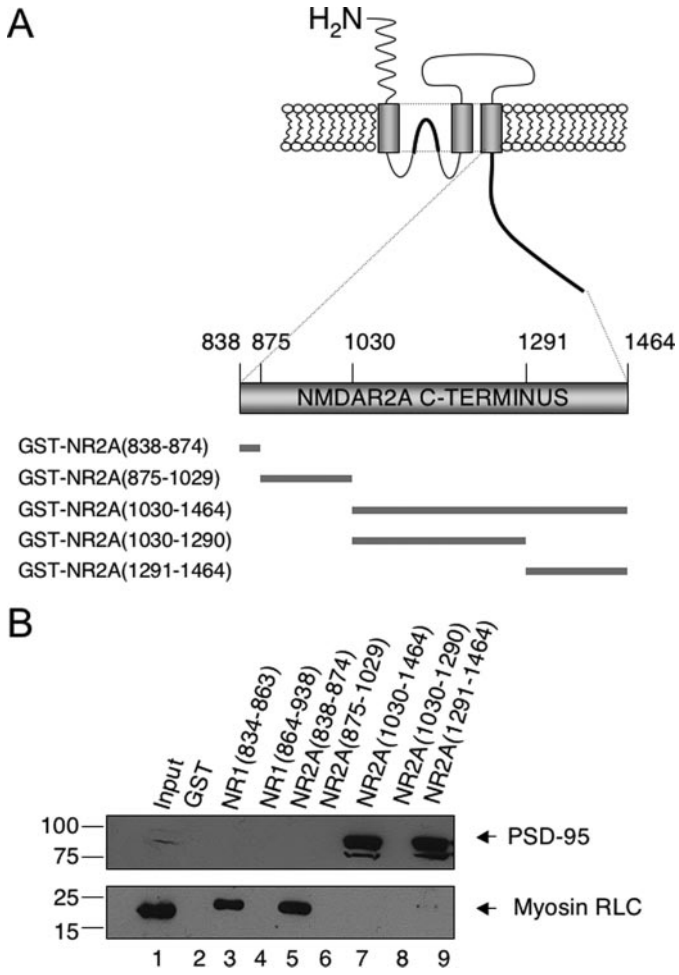

FIGURE 3. **Myosin RLC interacts with a short membrane-proximal region of the carboxyl-terminal domain of the NMDAR2A subunit.** *A,* schematic representation of NMDAR2A carboxyl-terminal deletion mutants used in *B*. *B,* deletion mutants of NR1 and NR2A carboxyl termini were fused to GST and used as baits to pull down native myosin RLC and a reference NMDA receptor-interacting protein (postsynaptic density protein of 95 kDa (PSD-95)) from mouse forebrain extract. Native myosin RLC was retained on the affinity matrices corresponding to the membrane-proximal region of NR2A-(838–874) and the membrane-proximal region of NR1-(834–863). Native PSD-95 was retained on NR2A affinity matrices containing only the extreme distal portion of the NR2A carboxyl terminus, consistent with recognized binding pattern of this protein (*B, lower panel*). GST fusion proteins, or GST alone, were immobilized on glutathione-Sepharose beads and incubated with rotation overnight at 4 °C with soluble forebrain extract (1 mg). Immune complexes corresponding to bound proteins were revealed with anti-myosin RLC (2) and anti-PSD95 antibodies (Abcam). Autoradiographs are representative of three independent determinations (from three different animals) using all seven NR mutants fused to GST; various combinations of NR2A mutants fused to GST were tested more frequently.

containing amino acids 1291–1464 of the NR2A carboxyl tail (Fig. 3*B, lane 9*). RLC binding, however, was not observed with the longer GST/NR2A-(1030–1464) mutant, suggesting that the interaction of native RLC with this distal portion of the NR2A subunit is either weak or possibly hindered by the presence of another NR2-interacting protein in mouse brain.

Multiple protein-protein interactions have now been documented at the level of glutamate receptor carboxyl termini (1). We therefore tested all GST affinity matrices concurrently for their ability to bind the known NR2-interacting protein, postsynaptic density protein of 95 kDa (PSD-95). Consistent with the NMDA receptor binding specificity of PSD-95 (38),

native mouse brain PSD-95 bound only to those mutants that contained the distal portions of the NR2A carboxyl tail (GST/NR2A-(1030–1464) and GST/NR2A-(1291–1464) (see Fig. 3*B, lanes 7* and *9* of *upper panel*). PSD-95 binds to a distal four amino acid motif (38), and thus our findings served to validate the use of a GST pulldown assay from mouse brain homogenates to map RLC-NMDA interactions. In agreement with our previous findings (2), myosin RLC bound specifically to a GST fusion protein containing the first 30 amino acids of the carboxyl terminus of the NR1 subunit (Fig. 3*B, lane 3*), yet failed to interact with either GST alone (*lane 2*) or a GST fusion protein containing the distal region (amino acid residues 864–938) of the NR1 carboxyl terminus (*lane 4*). In addition, native PSD-95 was not retained on control or GST/NR1 affinity matrices (Fig. 3*B, lanes 2–4*) indicating that PSD-95 displayed appropriate binding specificity in this assay.

Although NR1 and NR2 subunits of the NMDA receptor generally share low overall sequence homology (39), the membrane-proximal regions of the carboxyl terminus of both subtypes contain some conserved motifs that are primarily responsible for trafficking NMDA receptors to endocytic and degradative pathways (40, 41). We therefore expressed the membrane-proximal region of the NR2B subunit in bacteria as a GST fusion protein (GST/NR2B-(839–873)) to determine whether RLC also binds to this region of the NR2B subunit (alignment of all three subunits is shown in Fig. 4*A*). Native myosin RLC interacted strongly and specifically with GST/NR1- (834–863), GST/NR2A-(838–874), and GST/NR2B-(839–873) (Fig. 4*B*, *lanes 3, 5,* and *6* of *upper panel*) but failed to interact with the distal region of NR1-(864–938) (Fig. 4*B*, *lane 4*). Consistent with our previous findings with the NR1 subunit (2), none of the fusion proteins bound myosin ELC extracted from mouse brain even though this protein was also present in the homogenate (Fig. 4*B, lower panel*). Deletion of the membrane-proximal region of the NR2A carboxyl terminus by 7–20 amino acids (GST/NR2AΔ868 to GST/NR2AΔ855, Fig. 4*C*) abolished the interaction of RLC with NR2A (Fig. 4*D*, *lanes 6–8*). Taken together, these data indicate that RLC extracted from mouse brain binds to a membrane-proximal region of the carboxyl terminus of three major subunits of the NMDA receptor. The minimal RLC-binding site on the NR2A subunit is ~37 amino acids and is not a target for myosin ELC.

Membrane-proximal Regions of NR2A and NR2B Carboxyl Termini Are Not Targets for Calmodulin—Calmodulin is a resident light chain of some classes of the myosin motor. Calmodulin also modulates NMDA receptor function via a direct calcium-dependent interaction with the NR1 subunit (42, 43). We have previously shown that myosin RLC and Ca^{2+}/calmodulin share a common binding site on the membrane-proximal region of the NR1 subunit; myosin RLC was displaced by Ca^{2+}/calmodulin *in vitro* but was unaffected by calmodulin in the absence of calcium (2). To investigate the possibility of nonspecific interactions between EF-hand family proteins and NR2 subunits, we tested the ability of purified calmodulin to bind the membrane-proximal regions of NR2A and NR2B *in vitro*. These regions of the NR1, NR2A, and NR2B carboxyl termini were expressed in bacteria as GST fusion proteins and examined for interaction with purified calmodulin in the presence and absence of Ca^{2+} (Fig. 5). Calmodulin bound strongly and specifically to GST/NR1-(834–863) in the presence of Ca^{2+} (compare *lanes 3* and *8* in Fig. 5), yet failed to interact with the equivalent membrane-proximal regions of the NR2A (Fig. 5, *lanes 4* and *9*) and NR2B carboxyl termini (Fig. 5, *lanes 5* and *10*). These findings indicate that the first 34–36 amino acids of the NR2A and NR2B carboxyl termini do not harbor recognition sequences for calmodulin.

Myosin RLC Co-localizes with NMDAR2A in Whole Cells—We have previously shown that myosin RLC co-localizes with the NR1 subunit at dendritic sites in mature hippocampal neu-

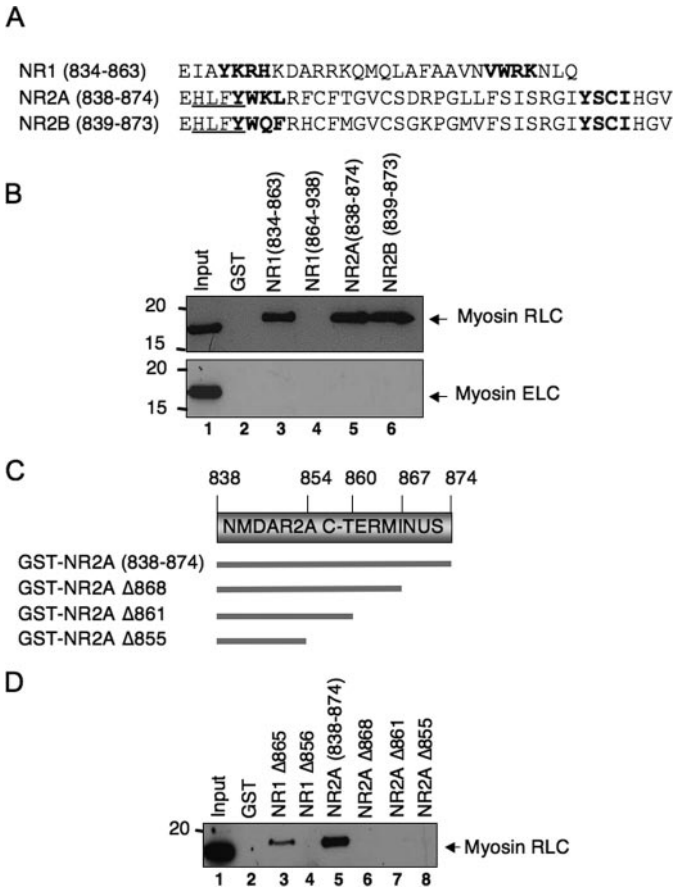

FIGURE 4. **The membrane-proximal carboxyl-terminal domain of three major NMDA receptor subunits harbors a binding site for myosin RLC.** *A,* amino acid alignment of the membrane-proximal regions of NR1, NR2A, and NR2B subunits; these regions were fused to GST and are represented in protein-protein interaction studies in *B*. The location of conserved endocytic motifs in all three subunits is shown in *boldface type*, whereas the location of an endoplasmic reticulum retention motif (HLFY) in NR2A and NR2B is *underlined*. *B,* membrane-proximal regions of NR1-(834–863), NR2A-(838–874), and NR2B-(839–873) pulldown myosin RLC but not a related EF-hand binding protein, myosin essential light chain (*ELC*), or from a mouse forebrain extract. *C,* schematic representation of NR2A carboxyl-terminal truncation mutants used in *D*. *D,* amino acids 838–874 in NR2A represent a minimal NR2A interaction domain. *B* and *D*, NR1-(834–863) corresponding to the C0 domain, NR1Δ856, NR1-(864–863), NR2A-(838–864), NR2B-(839–873), NR2AΔ868, NR2AΔ861, and NR2AΔ855 were expressed as GST fusion proteins. These GST fusion proteins, or GST alone, were immobilized on glutathione-Sepharose beads and used as baits to pull down myosin light chains from a mouse brain extract. Assays were initiated by the addition of soluble forebrain extract (1 mg) and incubated with rotation overnight at 4 °C. Bound proteins were resolved by PAGE and blotted to nitrocellulose; anti-myosin RLC (2) and anti-MLC1 (Abcam) antibodies were used to detect native RLC or ELC, respectively. Panels are representative of between three and five independent experiments from different animals.

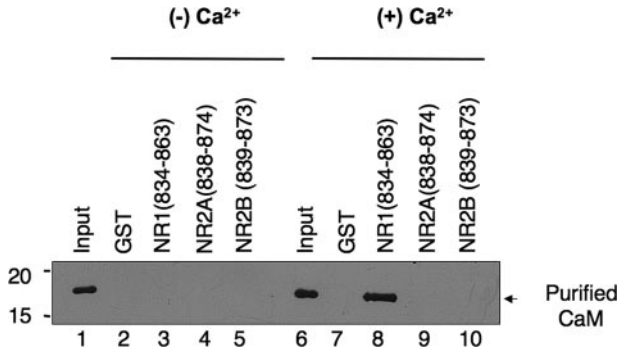

FIGURE 5. **The membrane-proximal carboxyl-terminal domains of NMDAR2A and NMDAR2B subunits do not bind calmodulin.** Calmodulin is structurally related to the myosin light chains yet does not bind NR2 subunits. The membrane-proximal region of NR1 was used as a positive control; NR1-(834–863) harbors one of two calmodulin-binding sites on the carboxyl terminus of the NR1 subunit that binds calmodulin in a strictly calcium-dependent manner. NR1-(834–863), NR2A-(838–874), and NR2B-(839–873) were expressed as GST fusion proteins, immobilized on glutathione-Sepharose beads, and tested for their ability to bind calmodulin in the absence (*lanes 1–5*) and presence (*lanes 6–10*) of calcium (2 mM). Assays were initiated by the addition of 500 nM calmodulin (Calbiochem) for 2 h at 4 °C in the presence and absence of calcium. Where appropriate, calcium (2 mM) was present throughout the experiment, including all wash buffers. Calmodulin bound to GST fusion proteins was resolved by PAGE and blotted to nitrocellulose. Immune complexes were detected using an anti-calmodulin antibody (Upstate Biotechnology, Inc.). Figure is representative of three independent experiments.

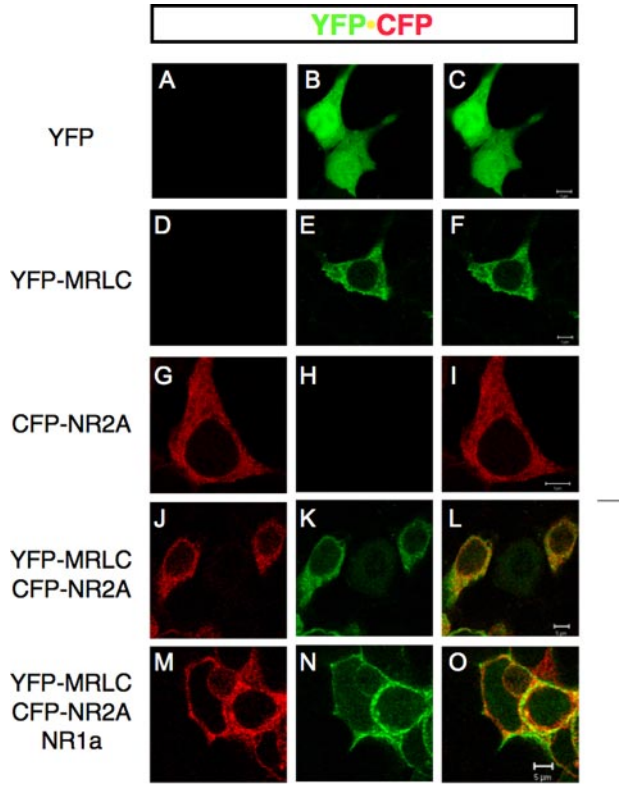

FIGURE 6. **The expression pattern of myosin RLC and NMDAR2A remains congruent in whole cells in the presence of NMDAR1.** Co-expression of a YFP-tagged myosin RLC and a CFP-tagged NR2A subunit in heterologous cells revealed considerable overlay of both proteins (see overlay of YFP and CFP signals in *L*). The expression pattern of YFP-myosin RLC (MRLC-YFP) and CFP-NR2A remained congruent in the presence of the NR1 subunit (see overlay of YFP and CFP signals in *O*; NR1a is untagged) but was redistributed to a membrane-associated domain. HEK293 cells grown on glass coverslips were transiently transfected with vector only (pEYFP-N1 is shown in *A–C*), a plasmid encoding full-length myosin RLC (MLC-YFP, *D–F*), a plasmid encoding NMDAR2A (1028-CFP, *G–I*), plasmids encoding myosin RLC plus NMDAR2A (MRLC-YFP + CFP-NR2A, *J–L*), or plasmids encoding myosin RLC, NMDAR2A plus NMDAR1 (MRLC-YFP + CFP-NR2A + NR1a, *M–O*). Confocal images were captured 48–72 h after each transfection, using a Zeiss LSM510 confocal microscope with a Zeiss 63× oil immersion objective. Fluorescence signals were collected using laser excitation at 514 nm for YFP and 458 nm for CFP; pseudocolor images were collected with LP 530 and BP 470–500 filters for detection of YFP (*1st column*) and CFP emission (*2nd column*), respectively. All cells were grown under standard conditions in medium supplemented with kynurenic acid (3 mM) and DL-AP5 (1 mM) to protect against cytotoxic cell death because of expression of functional recombinant NR1/NR2A receptors. Confocal images are representative of seven independent transfections. *Scale bar* = 5 μm.

rons grown in culture (2). Recombinant green fluorescent protein-tagged myosin RLC also localizes to postsynaptic sites in isolated hippocampal neurons (44). However, as all functional NMDA receptors are assemblies of NR1 and NR2 subunits, it is difficult to determine the possible significance of NR2A-RLC interaction in these studies. To provide some insight into the significance of myosin RLC-NR2A interactions in an intact cell, we took advantage of a heterologous expression system. Previous studies have shown that unassembled NR2 subunits are retained in the endoplasmic reticulum of heterologous cells and neurons by a short retention motif in the membrane-proximal region of the NR2 carboxyl terminus (Fig. 4*A*, *HLFY underlined*) and that cell surface expression of NR2 occurs only in the presence of the NR1 subunit (45). We therefore co-expressed myosin RLC and NR2A in HEK293 cells in the presence and absence of NR1. To avoid a potential second myosin RLC recognition site in the distal part of the carboxyl terminus (see Fig. 3), we used NR2A-(1–1028) for these studies as this NR2A deletion mutant has been characterized previously in HEK cells and forms a functional channel with normal physiological characteristics (46). In this study, expression of functional heteromeric NR1/CFP-NR2A-(1–1028) receptors was validated by the omission of glutamate receptor antagonists from the culture medium, which resulted in cell death (data not shown). Confocal fluorescence microscopy of HEK293 cells transiently expressing either myosin RLC fused to YFP or NR2A-(1–1028) fused to CFP (hereafter known as NR2A) revealed a predominant intracellular distribution of both proteins that could be clearly distinguished from that of YFP or CFP alone (Fig. 6, compare *YFP* alone in *A–C* with *D–F* and *G* to *H*; CFP alone is not shown). This cytoplasmic distribution was retained in HEK cells co-expressing YFP-RLC and CFP-NR2A (Fig. 6, *J* and *K*), as shown in an overlay of YFP and CFP channels (Fig. 6*L*). YFP-RLC and CFP-NR2A signals remained congruent in cells transfected with all three plasmids, yet the expression pattern was changed to a more peripheral membrane localization by the addition of the NR1 subunit (Fig. 6, *M–O*). Although these studies do not provide evidence of a direct interaction of myosin RLC with either NMDA receptor subunits, they suggest that a cytoskeletal rearrangement of myosin RLC and NR2A occurs in response to the presence of a functional NR1/NR2A assembly in intact cells.

Can Myosin RLC Bind to NMDA Receptor Subunits in the Context of a Myosin II Complex?—To determine whether a ternary complex could exist between myosin II heavy chain, the RLC, and NMDA receptor subunits, we tested the ability of recombinant NMIIB subfragment 1 (a myosin II heavy chain fragment that is already in a complex with RLC and ELC) to

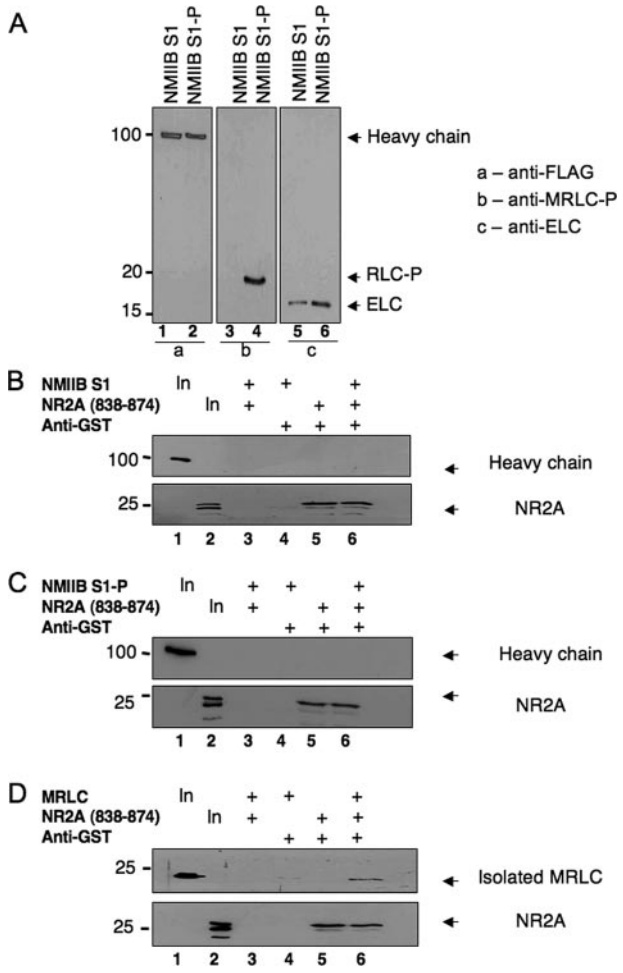

FIGURE 7. **Myosin RLC does not bind NMDAR2A in the context of either a phosphorylated or nonphosphorylated myosin II subfragment.** An NMIIB S1, consisting of a truncated heavy chain in complex with RLC and ELCs, did not form a ternary complex with NR2A. *A,* immunoblot analysis verifying phosphorylation of NMIIB S1 (*NMIIB S1-P*) by MLCK. Blots were probed with antibodies to all three components of the myosin II complex and are shown as follows: *panel a, lanes 1* and *2,* detection of heavy chain probed with an anti-FLAG antibody (Sigma); *panel b, lanes 3* and *4,* detection of phosphorylated myosin RLC (*RLC-P*) probed with a phospho-specific myosin RLC antibody raised in the laboratory; and *panel c, lanes 5* and *6,* detection of myosin ELC (*ELC*) probed with an anti-MLC1 antibody (Abcam). *B,* myosin II-B heavy chain (*upper panel*) is not precipitated with NR2A-(838–874) as a component of a nonphosphorylated NMIIB S1. *C,* myosin II-B heavy chain (*upper panel*) is not precipitated with NR2A-(838–874) as a component of MLCK-phosphorylated NMIIB S1. *D,* co-immunoprecipitation of recombinant MRLC with carboxyl-terminal NR2A-(838–938). For immunoprecipitation studies, purified GST-NR2A-(838–874) was incubated with nonphosphorylated NMIIB S1 (*B*), phosphorylated NMIIB S1 (*C*), or isolated myosin RLC (*D*) for 1 h at 4 °C in binding buffer (10 mM HEPES (pH 7.5), 100 mM NaCl, 1 mM EDTA, 1 mM dithiothreitol, 0.1% Nonidet P-40 and 10% glycerol). Protein complexes were then incubated with an anti-GST antibody and precipitated with protein G-Sepharose. Protein complexes were resolved by PAGE, transferred to nitrocellulose, and revealed by immunoblot analysis of NR2A and each component of the myosin II complex. The phosphorylation status of NMIIB was determined after each phosphorylation reaction; *B–D* are representative of at least three independent determinations.

bind to the membrane-proximal region of NR2A. Preliminary analyses indicated that all three components of NMIIB S1 complex (heavy, regulatory and essential light chains) could be identified independently either by Coomassie stain (not shown) or immunoblot analysis (Fig. 7*A*). Using an immunoprecipitation strategy, we tested the ability of NR2A-(838–874) fused to GST to form a complex with nonphosphorylated NMIIB S1 (Fig. 7*B*) or NMIIB S1 in which the RLC had been phosphorylated by MLCK (Fig. 7*C*). No precipitation of either form of NMIIB S1 was seen when NR2A-(838–874) was precipitated with an anti-GST antibody. Fig. 7, *B* and *C,* shows detection of myosin II heavy chain fragments in the input lane only (*lane 1, upper panels*), whereas control blots indicate that NR2A was precipitated by anti-GST (*lanes 5* and *6, lower panels*). An isolated myosin RLC was, however, co-immunoprecipitated with NR2A-(838–874) in parallel reactions; Fig. 7*D* shows positive identification of RLC (*lane 6, upper panel*) and NR2A (*lane 6, lower panel*) indicating that these two proteins were able to form a binary complex. Using conditions expected to favor NMDA receptor binding (*i.e.* physiological salt concentrations in the absence of magnesium), titration of NMIIB S1 (0–120 nM) produced a 100% increase in the fluorescence of the F-C0 peptide by 120 nM that was not saturable (data not shown). Taken together these data indicate that if RLC is already bound in the context of a myosin II complex, association with an NMDA receptor target protein likely represents a much lower affinity interaction than the interaction measured between NR1 and the isolated RLC.

Amino-terminal Region of Myosin RLC Is Critical for Interaction with NMDA Receptor Subunits—To determine which regions of myosin RLC are required for interaction with NMDA receptor subunits, we expressed several deletion mutants of RLC in bacteria (Fig. 8*A*) and examined them for interaction with either the carboxyl terminus of NR1 (Fig. 8*B*), the membrane-proximal region of NR2A (Fig. 8*C*), or the neck region of NMHC IIB (Fig. 8*D*) fused to GST, respectively. The RLC mutant corresponding to the first three helix-loop-helix motifs (or EF-hand domains) of the protein (residues 1–129) bound to GST/NR1 and GST/NR2A in a manner that was comparable with that of the full-length (residues 1–172) protein (Fig. 8*B*, compare *lanes 12* and *18* with Fig. 8*C*, *lanes 9* and *15*). The RLC mutant lacking the first EF-hand domain (residues 61–172) was also retained, albeit to a lesser extent, on a GST/NR1 affinity matrix (Fig. 8*B*, *lane 15*), but it was not retained on GST/NR2A (Fig. 8*C*, *lane 12*). Further deletion of either EF-hand domains three and four (residues 1–101), or EF-hand domains one and two (residues 102–172) abolished the interaction of myosin RLC with GST/NR1 and GST/NR2A (Fig. 8, *B* and *C lanes 3* and *6*, respectively). A mutant consisting of EF-hand domains two and three also failed to bind to NR1 (Fig. 8*B*, *lane 6*). In contrast to the pattern observed with NMDA receptor target sequences, all deletion mutants of myosin RLC failed to bind to NMHC IIB (Fig. 8*D*, *lanes 3, 6, 9,* and *12*). As shown in Fig. 8*D* (*lane 15*) only the full-length RLC was retained on the GST affinity matrix comprising the neck region of the myosin IIB heavy chain (residues 771–843). These findings indicate that the interaction of myosin RLC with NMDA receptor subunits may be structurally distinct from the classic RLC-heavy chain interaction. All regions of the light chain appear to be critical for binding to myosin II heavy chain. In contrast, the interaction of myosin RLC with NMDA receptor subunits requires residues in the amino terminus of the light chain and occurs in the absence of the fourth EF-hand domain.

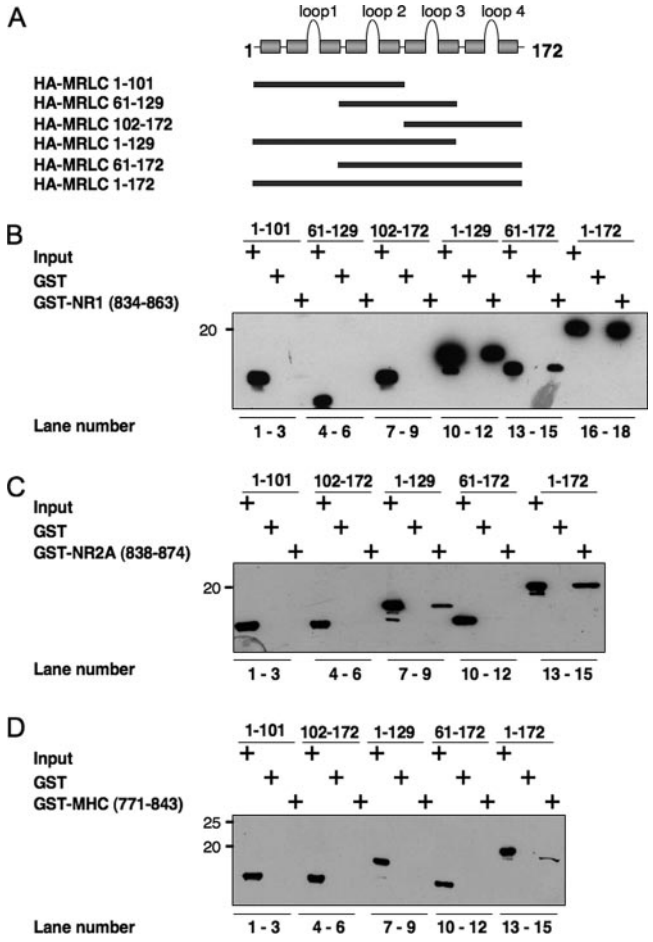

FIGURE 8. **The interaction of myosin RLC with NMDA receptor target sequences can be distinguished from RLC-heavy chain interactions.** *A,* schematic representation of a series of hemagglutinin (*HA*)-tagged myosin RLC deletion mutants used in *B–D*. *B,* truncated recombinant myosin RLC-(1–129) is sufficient for NR1-(834–938) binding (compare *lanes 12* and *18*). *C,* interaction of myosin RLC with NR2A-(834–874) is qualitatively similar to that of NR1, inasmuch as myosin RLC-(1–129) is sufficient for NR2A binding (compare *lanes 9* and *15*). *D,* full-length myosin RLC is necessary for binding non-muscle myosin II-B heavy chain (*MHC*); all deletion mutants of myosin RLC failed to bind the neck region of the heavy chain MHC-(771–843). Three RLC target sequences, NR1, NR2A, and myosin heavy chain, fused to GST, were tested for their ability to bind full-length and mutant RLCs. GST fusion proteins, or GST alone, were immobilized on glutathione-Sepharose beads and incubated at 4 °C with rotation overnight in the presence of 1 mM magnesium with either full-length (MRLC-(1–172)) or truncated light chains as follows: MRLC-(1–101), MRLC-(61–129), MRLC-(102–172), MRLC-(1–129), and MRLC-(61–172). Bound proteins were resolved by PAGE and blotted to nitrocellulose. Immune complexes were revealed by anti-T-7 antibody (Novagen). *B–D* are representative of three or four (NR2A) independent determinations.

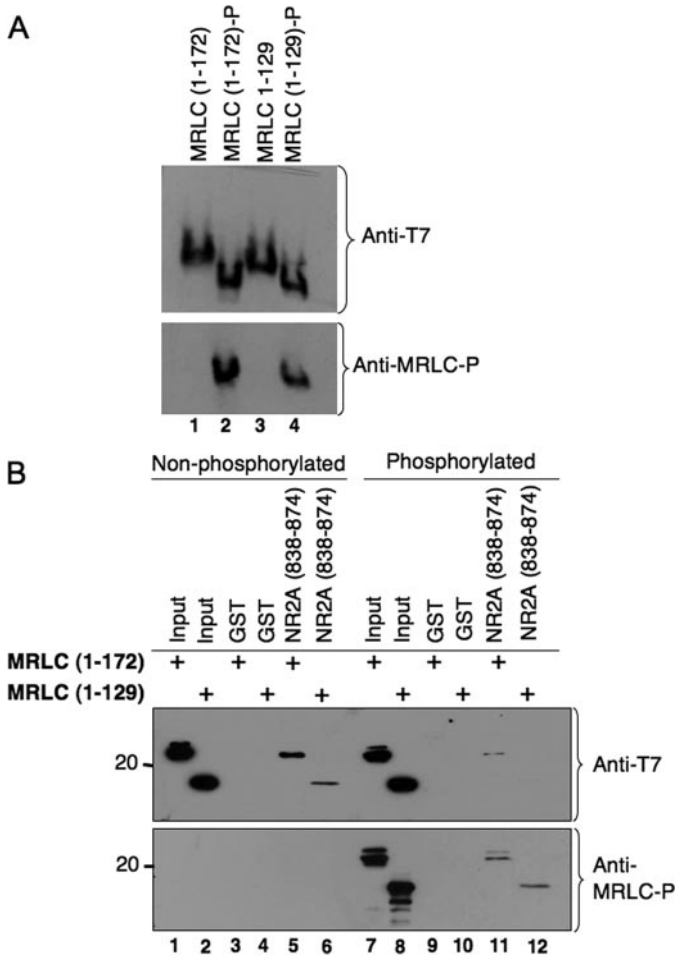

FIGURE 9. **Myosin RLC-NMDA receptor interactions are sensitive to phosphorylation by myosin light chain kinase.** *A,* phosphorylation of recombinant proteins by MLCK was verified after each reaction by PAGE in 8 M urea followed by Coomassie staining to visualize recombinant proteins. *A* shows representative immunoblot of full-length (residues 1–172) and truncated (residues 1–129) MRLC before (*lanes 1* and *3*) and after (*lanes 2* and *4*) phosphorylation by MLCK *in vitro*. *B,* following phosphorylation of RLC by MLCK, binding of myosin RLC to NR2A (residues 838–874) was decreased relative to the nonphosphorylated state. Purified proteins (MRLC-(1–172) and MRLC-(1–129)) were phosphorylated *in vitro* and used in GST pulldown experiments. NR2A-(838–874) fused to GST or GST alone was immobilized on glutathione-Sepharose beads and incubated with nonphosphorylated (*lanes 1–6*) or phosphorylated (*lanes 7–12*) forms of the isolated RLC at 4 °C with rotation for 2 h. Bound proteins were resolved by PAGE, transferred to nitrocellulose membranes, and probed with an anti-T-7 antibody (Novagen) capable of detecting both forms of the RLC (*upper panel*) or an anti-phospho-specific antibody raised in the laboratory (anti-MRLC-P; *lower panel*). *B* is representative of three independent determinations.

Myosin RLC Binding to the NMDA Receptor Is Sensitive to the Phosphorylation State of the Light Chain—The cyclical phosphorylation and dephosphorylation of myosin RLC represent a critical step in the actomyosin cycle of non-muscle and smooth muscle myosin II motors. To determine whether the interaction of myosin RLC with the NMDA receptor is influenced by phosphorylation of the light chain, we tested the ability of NR2A to bind full-length (residues 1–172) and mutant (residues 1–129) RLC phosphorylated by MLCK. By analogy to other RLCs, Thr-18 and Ser-19 are the likely targets of phosphorylation by MLCK. The extent of phosphorylation was first confirmed by urea-glycerol PAGE of RLCs followed by immunoblot analysis (Fig. 9*A*). Phosphorylated and nonphosphorylated RLCs were then examined for interaction with GST/NR2A-(838–874) using an antibody to both forms of the protein (Fig. 9*B*). Both the full-length and truncated (residues 1–129) light chains consistently showed reduced binding to NR2A in the phosphorylated state when compared with nonphosphorylated proteins (Fig. 9*B*, compare *lanes 5* and *6* with *lanes 11* and *12* of *upper panel*) or mock-phosphorylated proteins (data not shown). Binding of full-length and truncated RLC to NR2A was, however, revealed by the use of a phospho-specific antibody (Fig. 9*B*, *lower panel*). These findings indicate that phosphorylation of target residues in the amino terminus of the light chain disrupt binding to NR2A- (838–874). This

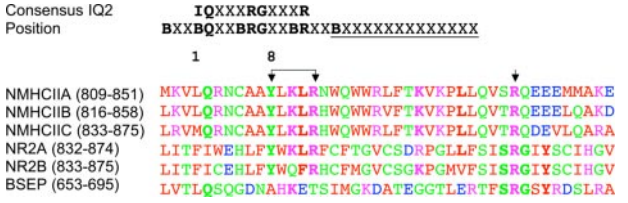

FIGURE 10. **Sequence alignment of putative RLC binding domains in non-muscle myosin heavy chain isoforms, NMDAR2 subunits, and bile salt export protein.** Amino acid sequences of incomplete IQ2 motifs in human non-muscle myosin II heavy chain isoforms as follows: II-A (accession number NP_002464), II-B (accession number NP_005955), and II-C (accession number Q7Z406), plus RLC-binding motif found in rat NMDAR2A (accession number NP_036705), NMDAR2B (accession numberAAA50554), and BSEP (accession number O70127). A consensus IQ2 motif is shown in *black*, where *B* indicates positions usually occupied by hydrophobic amino acids, and *X* is any amino acid. For non-muscle myosin heavy chain isoforms, the amino-terminal of myosin RLC is predicted to bind to a conserved target sequence WQWWRVFTKVKPLL for II-B, *underlined* in the consensus IQ2. *Arrows* indicate the following: the location of a tyrosine-based *YXXX*R motif beginning within the incomplete G*XXX*R portion of IQ2 that is conserved in all three heavy chains and both NMDA receptor subunits, and the location of an arginine residue that is conserved in all six myosin RLC targets. Standard single amino acid codes are used for all amino acid residues; residues are colored according to ClustalW (68), where *red* denotes small + hydrophobic (AVFPMILW), *blue* denotes acidic residues (DE), *magenta* denotes basic residues (RHK); and *green* denotes QSTYHCNG.

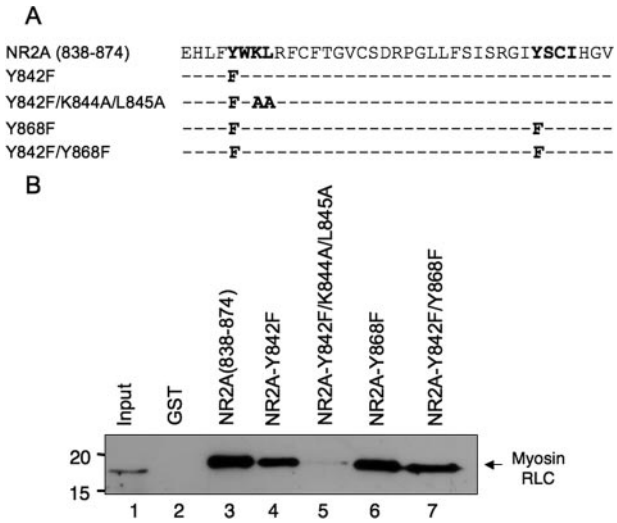

FIGURE 11. **Residues within a tyrosine-based endocytic motif associated with endocytosis of the NMDAR2A subunit are critical for myosin RLC binding.** *A,* schematic representation of site mutants used in *B*. The location of two tyrosine-based endocytic motifs within NR2A-(838–874) is shown in *boldface type*. The location of residues targeted for site-directed mutagenesis is listed *below* the wild-type sequence of NR2A. *B,* residues Lys-844 and Leu-845 in the membrane-proximal region of NR2A are critical for myosin RLC binding. NR2A-(838–874), NR2A-(838–874)Y842F, NR2A-(838–874)Y842F/K844A/L845A, NR2A-(838–874)Y868F, and NR2A-(838–874)Y842F/Y868F were expressed as GST fusion proteins. NR2A GST fusion proteins, or GST alone, were immobilized on glutathione-Sepharose beads and used as baits to pull down myosin light chains from a mouse brain extract. Assays were initiated by the addition of soluble forebrain extract (1 mg) and incubated with rotation overnight at 4 °C. Bound proteins were resolved by PAGE and blotted to nitrocellulose. Immune complexes were revealed using an anti-myosin RLC antibody (2). Autoradiographs are representative of three independent determinations (from three different animals) using all five NR mutants fused to GST; various combinations of NR2A mutants fused to GST were tested more frequently.

does not rule out the possibility that the light chain can remain bound to NR2A in the phosphorylated state.

Residues Lys-844 and Leu-845 in the Membrane-proximal Region of NR2A Are Critical for Myosin RLC Binding—The membrane-proximal regions of NMDA receptor subunits contain two tyrosine-based recognition sequences (Y*XXϕ*, where ϕ = a hydrophobic residue) for the clathrin-dependent, endocytic adapter protein 2 complex (AP-2) (40, 41) (see Fig. 4*A*). The neck region of smooth muscle and non-muscle myosin II heavy chains also contain a similar tyrosine-based sequence in the region of the neck that is considered an incomplete region of the IQ2 sequence (Fig. 10). For example, residues in positions 8, 10, and 11 of IQ2 of non-muscle II-B are identical to residues 842, 844, and 845 in the carboxyl terminus of NR2A (Fig. 10). We therefore used site-directed mutagenesis to target this Y*XX*KL motif in NR2A to determine whether these residues may be important for myosin RLC binding to the receptor (Fig. 11). Mutation of tyrosine residues 842 and 868 within NR2A (residues 838–874), either alone or together, produced no change in myosin RLC binding (Fig. 11*B*). Myosin RLC binding was lost, however, when the third and fourth positions of the first endocytic motif were also mutated to NR2A (Y842F/K844A/L845A) (Fig. 11*B*). None of the mutations tested affected the ability of the NR2A fusions to retain AP-2, which was detected using an antibody raised to the α subunit of the AP-2 complex (data not shown).

These data indicate that specific residues within the first membrane-proximal endocytic motif of NR2A are critical for myosin RLC binding. Sequence similarity between the membrane-proximal region of NR2 subunits and residues beginning at position 8 of the G*XXX*R portion of the incomplete IQ2 motif found in non-muscle myosin II heavy chain isoforms likely contributes to the recognition of NR2A as a non-myosin target of the RLC. Furthermore, alignment of three non-muscle myosin II heavy chains with the membrane-proximal regions of NR2A, NR2B, and the linker region of BSEP (as shown in Fig. 10) suggests that amino acid residues lying outside the typical IQ2 motif may contribute to recognition of non-myosin target sequences by the RLC.

Myosin RLC-NR2A Interactions Facilitate Forward Trafficking of NR1/NR2A Receptors—We disrupted amino acid residues 842, 844, and 845 in the context of CFP-NR2A and co-expressed NR2A(Y842F/K844A/L845A) (abbreviated to CFP-ΔNR2A) with NR1 and myosin RLC in HEK293 cells. Cells expressing the RLC-deficient NR2A showed dramatically delayed expression of membrane-associated CFP-ΔNR2A fluorescence when compared with control cells expressing wild-type NR2A (Fig. 12). Twenty four hours following transfection, CFP-ΔNR2A fluorescence appeared restricted to a discrete intracellular compartment in 73% of transfected cells, compared with the membrane-associated pattern of CFP-NR2A fluorescence anticipated in the presence of NR1 (Fig. 12, compare *A* with *D* and *G*). As the three amino acid tails required for exit of NR1/NR2A assemblies from the endoplasmic reticulum are intact in CFP-ΔNR2A (47), we stained transfected cells with an antibody raised to the Golgi-specific marker protein K58 (Fig. 12, *B* and *E*). Overlay of CFP-ΔNR2A and anti-K58 staining revealed CFP-ΔNR2A restricted to a sub-region of K58 positive staining within the cell (Fig. 12*F*). Intracellular CFP-ΔNR2A fluorescence (Fig. 12*G*) co-localized with YFP-RLC fluorescence (Fig. 12*H*) when observed 20–24 h post-transfec-

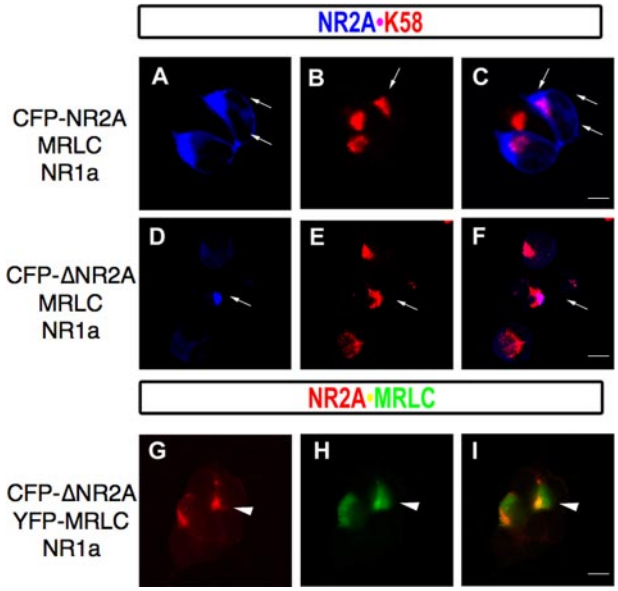

FIGURE 12. **Disruption of the myosin RLC-binding site on NMDAR2A leads to a trafficking defect in NR1/NR2A assemblies.** Co-expression of NR1, myosin RLC, and CFP-tagged NR2A (*A–C*) in heterologous cells revealed membrane-associated expression of CFP-NR2A 24 h post-transfection (*paired arrows* in *A* and *C*). In contrast, the RLC-deficient mutant CFP-ΔNR2A (CFP-NR2A-Y842F/K844A/L845A; *D–F*) showed a restricted cytosolic expression pattern within a region that was positive for the Golgi-specific marker protein K58 (*E* and *F*) at 24 h post-transfection. The restricted expression of CFP-ΔNR2A was congruent with YFP-myosin RLC (YFP-MRLC) despite the presence of NR1 (*G–I*) at 24 h post-transfection. In addition, a separate zone of YFP-myosin RLC fluorescence is also present (see *arrowhead, G–I*). HEK293 cells grown on glass coverslips were transiently transfected with plasmids encoding myosin RLC (MRLC), NMDAR1 (NR1a), and either wild-type NMDAR2A (*CFP-NR2A, A–C*)) or NMDAR2A-Y842F/K844A/L845A (*CFP-ΔNR2A, D–F*) and grown under standard conditions in medium supplemented with kynurenic acid (3 mM) and DL-AP5 (1 mM). Cells were fixed and counterstained with an anti-K58 antibody (Sigma) to visualize the Golgi complex ((*A–C* and *D–F*). Cells were also transfected with plasmids encoding NMDAR1 (NR1a), myosin RLC (YFP-MRLC), and either wild-type NMDAR2A (not shown) or NMDAR2A-Y842F/K844A/L845A (*CFP-ΔNR2A, G–I*). Confocal images were captured using a Zeiss LSM510 confocal microscope with a Zeiss 63× oil immersion objective. Confocal images are representative of at least three independent transfections. *Scale bar* = 5 μm.

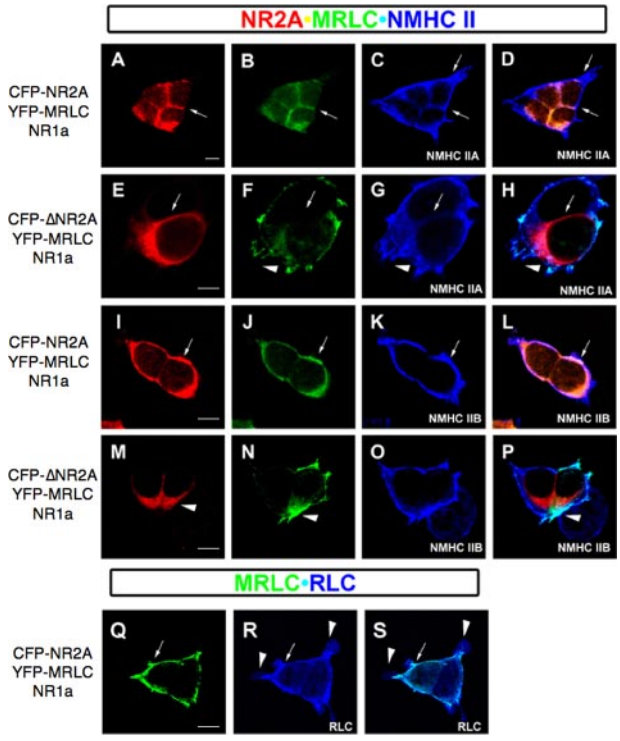

FIGURE 13. **Myosin RLC relocates to cellular extensions containing endogenous myosin heavy chain isoforms following disruption of NMDAR2A binding.** In the presence of a RLC-deficient NR2A mutant (CFP-NR2A-Y842F/K844A/L845A), the expression of RLC (YFP-MRLC) changes to a pattern that mimics myosin heavy chain II-A (see regions that appear *teal-colored* in *H*) or myosin heavy chain II-B (see regions that appear *teal-colored* in *P*). Although YFP-RLC fluorescence is not associated with all cellular extensions that contain myosin heavy chain (see *D* and *L*), these regions do contain an endogenous RLC (*arrowhead, R* and *Q*). HEK293 cells grown on glass coverslips were transiently transfected with plasmids encoding either wild-type NMDAR2A (*CFP-NR2A, A–D, I–L,* and *Q–S*) or NMDAR2A-Y842F/K844A/L845A (*CFP-ΔNR2A, E–H* and *M–P*), plus YFP-myosin RLC (YFP-MRLC) and NMDAR1 (NR1a) then grown under standard conditions in medium supplemented with kynurenic acid (3 mM) and DL-AP5 (1 mM). Thirty hours following transfection, cells were fixed and counterstained with isoform-specific antibodies to either non-muscle myosin heavy chain II-A (*A–D* and *E–H*), non-muscle myosin heavy chain II-B (*I–L* and *M–P*), or anti-myosin RLC (*Q–S*). Confocal images were captured using a Zeiss LSM510 confocal microscope with a Zeiss 63× oil immersion objective. Confocal images are representative of three to five independent transfections. *Scale bar* = 5 μm.

tion, shown in an overlay of YFP and CFP channels (Fig. 12*I*); however, YFP-RLC expression was also observed in the absence of CFP-ΔNR2A (Fig. 12*I*). When observed beyond 24 h after transfection, YFP-RLC and CFP-ΔNR2A signals were generally not congruent (Fig. 13, compare *E* and *F* and *M* and *N*). Consistent with a trafficking delay, cells expressing NR1/CFP-ΔNR2A receptors showed increased viability in the absence of glutamate receptor antagonists but were not protected from cell death (cells expressing NR1/CFP-ΔNR2A showed a 50% increase in viability at 72 h post-transfection compared with cells expressing NR1/CFP-NR2A, data not shown). In summary, myosin RLC-NR2A interactions likely occur within the Golgi secretory trafficking pathway. Disruption of RLC binding in intact cells led to altered NR2A expression and resulted in a delay in delivery of NR1/ΔNR2A receptors to the cell membrane.

Myosin RLC Co-localizes with Endogenous Myosin Heavy Chain following Disruption of the RLC Target Sequence in NR2A—To determine whether YFP-RLC fluorescence was associated with a myosin heavy chain, we stained transfected cells with isoform-specific antibodies raised to either NMHC-IIA or NMHC-IIB (Fig. 13). It was immediately apparent that both myosin heavy chain antibodies stained cellular extensions that showed neither YFP nor CFP fluorescence (Fig. 13, *A–C* and *I–K*). Overlay of all three channels revealed co-expression of YFP-RLC, CFP-NR2A, and a myosin heavy chain isoform in association with the cell membrane, in addition to cellular regions that stained only for NMCH-IIA (Fig. 13*D*) or NMCH-IIB (Fig. 13*L*). This pattern changed, however, if cells were transfected with the RLC-deficient mutant CFP-ΔNR2A (Fig. 13, *E–G* and *M* to *N*). Under these conditions cellular extensions showed YFP-RLC fluorescence that co-localized with NMCH-IIA (Fig. 13*H*) or NMCH-IIB (Fig. 13*P*) but not CFP-ΔNR2A fluorescence. These data indicate that an isolated RLC can localize to distinct subcellular compartments within an intact cell. Furthermore, YFP-RLC was not a component of all myosin II complexes in the cell, yet could re-localize to a previously unoccupied cellular compartment with a myosin heavy chain if binding to a non-myosin target, such as NR2A, was

disrupted. Localization of endogenous RLC in cellular extensions (Fig. 13*R*) not occupied by YFP-RLC (Fig. 13*Q*) or CFP-NR2A (omitted for clarity) was observed when cells were stained with an anti-myosin RLC antibody to reveal both expressed and native RLC. An overlay of both fluorescent signals (Fig. 13*S*) revealed YFP-RLC associated with the cell membrane (Fig. 13, *arrow* in *Q*–*S*) and native RLC (Fig. 13, *arrowhead* in *R* and *S*) presumably in complex with endogenous myosin II heavy chain.

DISCUSSION

Several unrelated myosin RLC-binding proteins have been reported in polarized epithelial cells and neurons, yet it is unclear how the prototypical myosin II motor complex interacts with these non-myosin targets. The identification of diverse myosin RLC targets raises the possibility that the RLC, like other EF-hand proteins, may adopt target-dependent conformations distinct from the conventional interaction of RLC with myosin II heavy chain. In this study we investigated the ability of a mouse brain myosin RLC to interact with NMDA-type glutamate receptor subunits. We characterized the molecular determinants that underlie direct binding of myosin II RLC to the membrane-proximal carboxyl-terminal regions of NR1 and NR2 glutamate receptor subunits. The interaction of RLC with NMDA receptor subunits was fundamentally different from the typical interaction of the light chain with the neck region of myosin II heavy chain; NMDA receptor-RLC interactions did not require the addition of magnesium, were maintained in the absence of the fourth EF-hand domain of the light chain, and were sensitive to RLC phosphorylation by MLCK. Thus, our data support a model whereby the RLC forms a distinct complex with either NR1 or NR2 subunits that essentially serve as the "heavy chain." Finally, subcellular fluorescence microscopy studies reveal co-localization of myosin RLC with NR2 subunits and subsequent re-localization of both proteins in response to NR1 co-expression to form a functional NMDA receptor channel. Myosin RLC-NR2A interactions were functionally significant, inasmuch as cells expressing an RLC-deficient NR2A subunit showed a trafficking defect in the presence of NR1. Together these findings suggest a role for myosin RLC independent of the myosin complex.

We defined a myosin RLC-binding site on three NMDA receptor subunits that was restricted to a 30–37-amino acid stretch directly following the fourth hydrophobic domain of each NR2A subunit. This region is functionally equivalent in NR1 and NR2 subunits in that it contains tyrosine-based recognition motifs for endocytosis of the receptor (40, 41). These membrane-proximal regions lack conserved IQ motifs that are normally associated with myosin light chain or apo-calmodulin binding; however, the C0 region of the NR1 subunit harbors a non-IQ, atypical CaM-binding site that binds Ca^{2+}-CaM as well as myosin RLC. The relatively high affinity (~30 nM) of myosin RLC for the C0 region of NR1 was comparable with binding affinities derived previously for Ca^{2+}-CaM binding to C0 *in vitro*, reported as 87 nM (42) and 21 nM (43) by two different groups. Although apo-calmodulin associates with C0 *in vitro* (2, 48), it does so with relatively modest affinity in the absence of calcium (K_D = 2.5 μM) (48). Thus the affinity of myosin RLC for C0, in the absence of calcium, is comparable with the affinity of Ca^{2+}-CaM for this site. Overlapping myosin RLC- and CaM-binding sites have been described previously in the RLC-interacting protein calponin. Unlike NR1, the membrane-proximal regions of NR2A and NR2B represent RLC target sequences that do not bind apo-CaM, Ca^{2+}-CaM, or myosin ELC. Thus the NR2 subunits potentially represent RLC-interacting proteins requiring novel RLC structural conformations, and for this reason formed the focus of our study.

Our studies support a role for only three of the four EF hand domains as necessary for RLC binding to NMDA receptor subunits. However, we were unable to isolate a stable, high affinity ternary complex *in vitro* that, in theory, could be formed if the fourth EF hand domain remained free to bind myosin heavy chain. Instead our data support a model whereby the RLC forms a distinct complex with either NR1 or NR2 subunits that interact in lieu of the heavy chain. Such a scenario would not necessarily require a large pool of free light chain as local physiological conditions, for example divalent cation concentration and/or the phosphorylation status of the RLC, may favor transition between one binding partner over another.

Our findings with brain myosin RLC are reminiscent of the *S. cerevisiae* light chain Mlc1p, in that Mlc1p forms independent complexes with myosin II and IQGAP; Mlc1p-Myo1p (myosin II) interactions can be separated from Mlc1p-IQGAP interactions (16). All three proteins can be isolated in a biochemical complex and co-localize in cells during late mitosis, yet Mlc1p does not form a bridge between IQGAP and Myo1p (16). As a working model, we propose that RLC forms a distinct complex with NMDA receptor subunits and also with myosin II heavy chain. By analogy to Mlc1p, such an interaction could serve to recruit the NMDA receptor and a myosin II motor sequentially to a specialized subcellular compartment in a neuron. This model takes into account our biochemical characterization of direct NMDA-RLC interactions, as well as the work of others showing that a non-muscle myosin II-B motor complex is closely associated with the NMDA-type glutamate receptor (2, 49–52).

Although several RLC-interacting proteins have been described in the literature (2, 19, 20, 24), there is currently no unifying mechanism to explain how a myosin II RLC could bind simultaneously to a myosin II heavy chain and a second target protein such as MIR, an NMDA receptor subunit, or an ABC transporter. It has been proposed that calponin binds F-actin and the phosphorylated form of RLC, in the context of a myosin II complex, to regulate smooth muscle contractility (53). Calcium appears to be a central regulator of this interaction; myosin RLC is phosphorylated by the Ca^{2+}-CaM-dependent enzyme MLCK, and the interaction between F-actin and calponin may be disrupted by Ca^{2+}-CaM (19, 53). This is intriguing as NMDA receptor subunits bind directly to myosin RLC and are also physically "latched" to F-actin at postsynaptic sites by actin-binding proteins such as α-actinin-2 and spectrin (54, 55). The NMDA receptor is a ligand-gated calcium channel and thus some functional parallels can be drawn with the calponin interaction in smooth muscle. Ca^{2+}-CaM competes for myosin RLC and α-actinin-2 binding sites on the C0 region of NR1 (55).

The direct binding of Ca^{2+}-CaM to the C0 region of NR1 results in a reversible calmodulin-dependent inactivation of NMDA receptor channels (43, 56), some characteristics of which can be recapitulated in hippocampal neurons by direct manipulation of MLCK (50).

Myosin RLC-NMDA receptor interactions were sensitive to the phosphorylation state of the light chain, in that phosphorylation of RLC by MLCK decreased receptor binding relative to the unphosphorylated RLC. These findings are consistent with a role for the amino portion of the light chain as a determinant of NMDA receptor binding, as the expected targets for phosphorylation by MLCK, threonine 18 and serine 19, are located within this region (3). Our ability to detect phosphorylated myosin RLC bound to NMDA receptor targets was not surprising inasmuch as the RLC remains bound to the heavy chain neck throughout the actin myosin ATPase cycle. These studies revealed a potentially important similarity between the interaction of RLC with NMDA receptor subunits and the smooth muscle protein calponin (19), in that the amino terminus of the light chain is important for binding to both non-myosin targets. In contrast to the reported interaction of calponin with RLC (53), the phosphorylated form of RLC was not favored in our studies. Taken together, these protein-protein interaction studies indicate that the RLC adopts a conformation with the NMDA receptor that can be distinguished from the interaction of RLC with its normal binding partner, myosin II heavy chain. The disposition of myosin RLC in binding MIR or ABC transporters such as BSEP remains to be determined.

Despite some common themes, we saw no evidence for binding of either unphosphorylated or phosphorylated myosin RLC to NR2A in the context of a recombinant NMIIB subfragment 1. These studies were carried out in physiological salt concentrations capable of detecting direct binding of proteins such as PSD-95 or Ca^{2+}-CaM to the receptor. In addition, the fluorescence signal arising from the C0 peptide upon titration of subfragment 1 was not easily saturable, indicating that the affinity of myosin RLC for NR1 in the context of the myosin subfragment would be significantly lower than the nanomolar affinity measured for the isolated light chain. These kinds of studies are, however, technically challenging *in vitro* as the solubility and stability of the myosin II subfragment is also compromised at physiological salt concentrations. Although it is not possible to rule out a transient calponin-like interaction between the receptor and a neuronal myosin II *in vivo*, it seems most likely that binding of a third target protein is not favored once the RLC is already in a complex with myosin II heavy chain.

The current understanding of conventional myosin II structure therefore does not explain how an RLC could bind to two target proteins simultaneously. Structural studies have revealed that the RLC always binds to the neck region of myosin II heavy chain in an open and extended conformation. In fact the amino terminus of RLC binds to a highly conserved tryptophan-rich target sequence that is not actually part of the IQ2 motif, whereas the carboxyl terminus binds to the IQ*XXX*R portion of the incomplete IQ2 located in the myosin heavy chain (8). Site-directed mutagenesis of residues within the NR2A target sequence, however, revealed that the most likely explanation for recognition of NR2 subunits as non-myosin targets was because of sequence homology between NR2 and residues within the neck region of myosin II that are not part of the canonical IQ2 motif. These findings illustrate that a protein need not contain consensus IQ motifs to be a target of the isolated RLC. This is important as screening for the presence of IQ motifs has been employed as a strategy for uncovering new binding targets of highly related EF-hand-containing proteins.

It is becoming accepted that myosin ELC has binding partners other than the myosin II heavy chain. This viewpoint has been facilitated by clear differences in the spatial and temporal distribution and/or stability of the ELC *versus* RLC and myosin II heavy chain in organisms such as *Dictyostelium* (57), the yeasts *S. cerevisiae* and *S. pombe* (13, 16, 17), and *D. melanogaster* (11). These kinds of studies are more difficult in the mammalian central nervous system as expression of components of the myosin II complex is under the control of more than one gene, thus making it difficult to track each polypeptide. For example, three separate genes encode non-muscle myosin II heavy chain isoforms (II-A, II-B, and II-C) (3), and at least two of these (II-B and II-C) are alternately spliced (58, 59). Several RLC isoforms have also been described in brain (34–36), yet it is not clear if particular light chain isoforms are shared by more than one heavy chain or if the pairing of RLC light chain and heavy chain II isoforms is isoform-specific. Our present findings indicate that a brain RLC can localize with either myosin II-B or II-A heavy chain isoforms when binding to a non-myosin target is disrupted. Differential staining patterns observed with RLC and non-muscle myosin II-B heavy chain antibodies in brain also indicate that heterogeneity in the composition of native myosin II complexes is likely, despite comparable expression of RLC, ELC, and NMHC-IIB in mouse cortex, hippocampus, and cerebellum (52). In *D. melanogaster,* which has a single gene encoding the ELC (essential light chain-cytoplasmic), RLC (spaghetti squash), and heavy chain (zipper), at least four alternate binding partners for the ELC have been identified (11). However, all three components of the myosin II complex appear to be expressed in relatively constant stoichiometric amounts, and by far the majority of both light chains is bound to myosin II heavy chain; using an immunodepletion strategy greater than 90% of ELC and greater than 95% of RLC were bound to myosin II heavy chain in wild-type embryos (11). These authors conclude that although the majority of both light chains are associated with non-muscle myosin II heavy chain, pools of free light chain and/or light chain bound to other proteins are present (11). These findings illustrate the potential challenges in studying either alternate binding partners or free pools of myosin light chains in the mammalian brain.

The expression pattern of YFP-myosin RLC in HEK cells showed significant overlay with that of the NR2A subunit when expressed either alone or in the context of a heteromeric membrane-bound NR1/NR2A receptor. We used site-directed mutagenesis to disrupt co-localization of NR2A with the light chain and to identify the Golgi complex as a specific region within the cell where RLC interactions may be functionally important in forward trafficking of NR1/NR2A receptors. The cytosolic localization of myosin RLC and NR2A in cells is consistent with our previous observation that native myosin RLC is

co-expressed with the NR1 subunit in the soma of some neuronal populations in neonatal and adult mice (52). A punctate, perinuclear staining pattern corresponding to overlapping NR1 and myosin RLC immunoreactivity was clearly observed in the soma of deep cortical neurons and in Purkinje neurons of the cerebellum (52). Although the exact intracellular compartment remains to be identified, the simplest explanation for the observed expression patterns in cells and neurons is that myosin RLC is closely associated with NMDA receptor subunits early in the secretory pathway before delivery from the Golgi to postsynaptic sites. In the case of the ABC transporter BSEP, a direct binding partner of RLC, it has been proposed that myosin RLC is required for trafficking of newly synthesized BSEP to the apical membrane and/or the release of BSEP vesicles from the trans-Golgi network of hepatocytes (20, 60). Myosin II binds to the Golgi membrane via the tail domain of the heavy chain, leaving the head region free to interact with F-actin. In this orientation, myosin II is thought to move Golgi-derived vesicles away from the Golgi complex (61). Our finding that non-muscle myosins IIB and Va are, like NMDA receptor subunits, raft-associated proteins (62), is consistent with the general hypothesis that affinity for lipid rafts can provide a sorting platform for exit from the trans-Golgi network in polarized cells (63). The specific mechanisms responsible for movement and export of NMDA receptor-containing vesicles from the Golgi are not clear; however, microtubule-based motors subsequently play a role in trafficking NMDA receptor transport packets to the vicinity of a new postsynaptic site (64). The kinesin family member KIF17 has been reported to associate with the NR2B subunit; however, NR2B trafficking by this particular molecular motor occurs at the level of the dendritic shaft, and KIF17 does not enter the actin-rich dendritic spine (65). Dendritic spines are largely devoid of microtubules, and thus it is unlikely that microtubule-based motors are responsible for movement and trafficking of NMDA receptor complexes within the spine itself. Although proteomic analyses have identified members of the myosin superfamily representing classes I, II, V, VI, and XVIII at glutamate synapses (66, 67), the functional significance of this observation is not yet appreciated.

In this study, we observed significant re-localization of NR2A and myosin RLC in heterologous cells in the presence of the NR1 subunit. Receptors containing an RLC-deficient NR2A subunit showed a temporal trafficking defect, indicating that more than one mechanism for trafficking NR1/NR2A assemblies is present in HEK cells. The apparent redistribution of RLC and wild-type NR2A proteins to a membrane-associated domain is consistent with previous studies in mature hippocampal neurons that show native myosin RLC is located at dendritic spines with NMDA receptors. Green fluorescent protein-tagged myosin RLC has also been shown by others to localize to the dendritic spines of transfected hippocampal neurons (44). Our findings in intact cells therefore extend our previous observations in that myosin RLC appears to be associated with the NR2A subunit, a second marker of functional NMDA receptors, as well as the NR1 subunit. By analogy to our current understanding of the role of RLC in BSEP trafficking in polarized epithelial cells (20, 60), the following two possible regions of interest emerge as being potential locations for direct and/or indirect interactions between the NMDA receptor, the RLC, and a neuronal myosin II motor: 1) an endomembrane compartment within the neuronal soma that is likely associated with the Golgi apparatus, and 2) a postsynaptic compartment corresponding to the dendritic spine. With respect to the direct interaction of RLC with NMDA receptor subunits, we suggest that myosin RLC has the ability to adopt target-dependent conformations with non-myosin binding partners in the absence of a heavy chain to fulfill a trafficking function.

Acknowledgments—We thank Dr. Jim Sellers (National Institutes of Health, Bethesda) for the generous gift of recombinant non-muscle II-B subfragment 1. We also thank Anne-Marie Gerard and Tamara Fraley for assistance with confocal imaging and Dr. Jeff Greenwood, Dr. Christopher Thomas, and Dr. Gary Westbrook for helpful discussions. We thank the Research and Scholarship Fund of the Oregon State University College of Pharmacy for the purchase of the fluorescent NR1 peptide.

REFERENCES

1. Wenthold, R. J., Prybylowski, K., Standley, S., Sans, N., and Petralia, R. S. (2003) *Annu. Rev. Pharmacol. Toxicol.* **43,** 335–358
2. Amparan, D., Avram, D., Thomas, C. G., Lindahl, M. G., Yang, J., Bajaj, G., and Ishmael, J. E. (2005) *J. Neurochem.* **92,** 349–361
3. Conti, M. A., and Adelstein, R. S. (2008) *J. Cell Sci.* **121,** 11–18
4. Kawasaki, H., Nakayama, S., and Kretsinger, R. H. (1998) *Biometals* **11,** 277–295
5. Bahler, M., and Rhoads, A. (2002) *FEBS Lett.* **513,** 107–113
6. Houdusse, A., and Cohen, C. (1995) *Proc. Natl. Acad. Sci. U. S. A.* **92,** 10644–10647
7. Terrak, M., Otterbein, L. R., Wu, G., Palecanda, L. A., Lu, R. C., and Dominguez, R. (2002) *Acta Crystallogr. Sect. D Biol. Crystallogr.* **58,** 1882–1885
8. Terrak, M., Wu, G., Stafford, W. F., Lu, R. C., and Dominguez, R. (2003) *EMBO J.* **22,** 362–371
9. Rayment, I., Rypniewski, W. R., Schmidt-Base, K., Smith, R., Tomchick, D. R., Benning, M. M., Winkelmann, D. A., Wesenberg, G., and Holden, H. M. (1993) *Science* **261,** 50–58
10. Houdusse, A., and Cohen, C. (1996) *Structure* (*Lond.*) **4,** 21–32
11. Franke, J. D., Boury, A. L., Gerald, N. J., and Kiehart, D. P. (2006) *Cell Motil. Cytoskeleton* **63,** 604–622
12. Stevens, R. C., and Davis, T. N. (1998) *J. Cell Biol.* **142,** 711–722
13. Luo, J., Vallen, E. A., Dravis, C., Tcheperegine, S. E., Drees, B., and Bi, E. (2004) *J. Cell Biol.* **165,** 843–855
14. Bezanilla, M., Forsburg, S. L., and Pollard, T. D. (1997) *Mol. Biol. Cell* **8,** 2693–2705
15. Espindola, F. S., Suter, D. M., Partata, L. B., Cao, T., Wolenski, J. S., Cheney, R. E., King, S. M., and Mooseker, M. S. (2000) *Cell Motil. Cytoskeleton* **47,** 269–281
16. Boyne, J. R., Yosuf, H. M., Bieganowski, P., Brenner, C., and Price, C. (2000) *J. Cell Sci.* **113,** 4533–4543
17. Shannon, K. B., and Li, R. (2000) *Curr. Biol.* **10,** 727–730
18. Weissbach, L., Bernards, A., and Herion, D. W. (1998) *Biochem. Biophys. Res. Commun.* **251,** 269–276
19. Szymanski, P. T., and Goyal, R. K. (1999) *Biochemistry* **38,** 3778–3784
20. Chan, W., Calderon, G., Swift, A. L., Moseley, J., Li, S., Hosoya, H., Arias, I. M., and Ortiz, D. F. (2005) *J. Biol. Chem.* **280,** 23741–23747
21. Nagano, K., Bornhauser, B. C., Warnasuriya, G., Entwistle, A., Cramer, R., Lindholm, D., and Naaby-Hansen, S. (2006) *EMBO J.* **25,** 1871–1882
22. Bornhauser, B. C., Johansson, C., and Lindholm, D. (2003) *FEBS Lett.* **553,** 195–199
23. Olsson, P. A., Bornhauser, B. C., Korhonen, L., and Lindholm, D. (2000) *Biochem. Biophys. Res. Commun.* **279,** 879–883
24. Olsson, P. A., Korhonen, L., Mercer, E. A., and Lindholm, D. (1999) *J. Biol.*

Chem. **274,** 36288–36292
25. Knowlton, M. N., and Kelly, G. M. (2004) *Zebrafish* **1,** 133–144
26. Knowlton, M. N., Chan, B. M., and Kelly, G. M. (2003) *Dev. Biol.* **264,** 407–429
27. Ishmael, J. E., Franklin, P. H., Murray, T. F., and Leid, M. (1996) *J. Neurochem.* **67,** 1500–1510
28. Malencik, D. A., and Anderson, S. R. (1982) *Biochemistry* **21,** 3480–3486
29. Malencik, D. A., and Anderson, S. R. (1988) *Biochemistry* **27,** 1941–1949
30. Wang, F., Kovacs, M., Hu, A., Limouze, J., Harvey, E. V., and Sellers, J. R. (2003) *J. Biol. Chem.* **278,** 27439–27448
31. Cremo, C. R., Wang, F., Facemyer, K., and Sellers, J. R. (2001) *J. Biol. Chem.* **276,** 41465–41472
32. Krupp, J. J., Vissel, B., Thomas, C. G., Heinemann, S. F., and Westbrook, G. L. (2002) *Neuropharmacology* **42,** 593–602
33. Zhang, Y., Vogel, W. K., McCullar, J. S., Greenwood, J. A., and Filtz, T. M. (2006) *Mol. Pharmacol.* **70,** 860–868
34. Taubman, M. B., Grant, J. W., and Nadal-Ginard, B. (1987) *J. Cell Biol.* **104,** 1505–1513
35. Feinstein, D. L., Durand, M., and Milner, R. J. (1991) *Brain Res. Mol. Brain Res.* **10,** 97–105
36. Wang, Y., and Chantler, P. D. (1994) *FEBS Lett.* **348,** 244–248
37. Zavodny, P. J., Petro, M. E., Kumar, C. C., Dailey, S. H., Lonial, H. K., Narula, S. K., and Leibowitz, P. J. (1988) *Nucleic Acids Res.* **16,** 1214
38. Kornau, H. C., Schenker, L. T., Kennedy, M. B., and Seeburg, P. H. (1995) *Science* **269,** 1737–1740
39. Monyer, H., Sprengel, R., Schoepfer, R., Herb, A., Higuchi, M., Lomeli, H., Burnashev, N., Sakmann, B., and Seeburg, P. H. (1992) *Science* **256,** 1217–1221
40. Vissel, B., Krupp, J. J., Heinemann, S. F., and Westbrook, G. L. (2001) *Nat. Neurosci.* **4,** 587–596
41. Scott, D. B., Michailidis, I., Mu, Y., Logothetis, D., and Ehlers, M. D. (2004) *J. Neurosci.* **24,** 7096–7109
42. Ehlers, M. D., Zhang, S., Bernhadt, J. P., and Huganir, R. L. (1996) *Cell* **84,** 745–755
43. Krupp, J. J., Vissel, B., Thomas, C. G., Heinemann, S. F., and Westbrook, G. L. (1999) *J. Neurosci.* **19,** 1165–1178
44. Zhang, H., Webb, D. J., Asmussen, H., Niu, S., and Horwitz, A. F. (2005) *J. Neurosci.* **25,** 3379–3388
45. Hawkins, L. M., Prybylowski, K., Chang, K., Moussan, C., Stephenson, F. A., and Wenthold, R. J. (2004) *J. Biol. Chem.* **279,** 28903–28910
46. Vissel, B., Krupp, J. J., Heinemann, S. F., and Westbrook, G. L. (2002) *Mol. Pharmacol.* **61,** 595–605
47. Yang, W., Zheng, C., Song, Q., Yang, X., Qiu, S., Liu, C., Chen, Z., Duan, S., and Luo, J. (2007) *J. Biol. Chem.* **282,** 9269–9278
48. Akyol, Z., Bartos, J. A., Merrill, M. A., Faga, L. A., Jaren, O. R., Shea, M. A., and Hell, J. W. (2004) *J. Biol. Chem.* **279,** 2166–2175
49. Husi, H., Ward, M. A., Choudhary, J. S., Blackstock, W. P., and Grant, S. G. (2000) *Nat. Neurosci.* **3,** 661–669
50. Lei, S., Czerwinska, E., Czerwinski, W., Walsh, M. P., and MacDonald, J. F. (2001) *J. Neurosci.* **21,** 8464–8472
51. Ryu, J., Liu, L., Wong, T. P., Wu, D. C., Burette, A., Weinberg, R., Wang, Y. T., and Sheng, M. (2006) *Neuron* **49,** 175–182
52. Kioussi, C., Appu, M., Lohr, C. V., Fischer, K. A., Bajaj, G., Leid, M., and Ishmael, J. E. (2007) *Brain Res. Bull.* **74,** 439–451
53. Szymanski, P. T. (2004) *J. Muscle Res. Cell Motil.* **25,** 7–19
54. Wechsler, A., and Teichberg, V. I. (1998) *EMBO J.* **17,** 3931–3939
55. Wyszynski, M., Lin, J., Rao, A., Nigh, E., Beggs, A. H., Craig, A. M., and Sheng, M. (1997) *Nature* **385,** 439–442
56. Zhang, S., Ehlers, M. D., Bernhardt, J. P., Su, C. T., and Huganir, R. L. (1998) *Neuron* **21,** 443–453
57. Maeda, M., Kuwayama, H., Yokoyama, M., Nishio, K., Morio, T., Urushihara, H., Katoh, M., Tanaka, Y., Saito, T., Ochiai, H., Takemoto, K., Yasukawa, H., and Takeuchi, I. (2000) *Dev. Biol.* **223,** 114–119
58. Takahashi, M., Kawamoto, S., and Adelstein, R. S. (1992) *J. Biol. Chem.* **267,** 17864–17871
59. Golomb, E., Ma, X., Jana, S. S., Preston, Y. A., Kawamoto, S., Shoham, N. G., Goldin, E., Conti, M. A., Sellers, J. R., and Adelstein, R. S. (2004) *J. Biol. Chem.* **279,** 2800–2808
60. Wakabayashi, Y., Kipp, H., and Arias, I. M. (2006) *J. Biol. Chem.* **281,** 27669–27673
61. Fath, K. R. (2005) *Cell Motil. Cytoskeleton* **60,** 222–235
62. Ishmael, J. E., Safic, M., Amparan, D., Vogel, W. K., Pham, T., Marley, K., Filtz, T. M., and Maier, C. S. (2007) *Brain Res.* **1143,** 46–59
63. Zegers, M. M., and Hoekstra, D. (1998) *Biochem. J.* **336,** 257–269
64. Washbourne, P., Bennett, J. E., and McAllister, A. K. (2002) *Nat. Neurosci.* **5,** 751–759
65. Guillaud, L., Setou, M., and Hirokawa, N. (2003) *J. Neurosci.* **23,** 131–140
66. Cheng, D., Hoogenraad, C. C., Rush, J., Ramm, E., Schlager, M. A., Duong, D. M., Xu, P., Wijayawardana, S. R., Hanfelt, J., Nakagawa, T., Sheng, M., and Peng, J. (2006) *Mol. Cell. Proteomics* **5,** 1158–1170
67. Collins, M. O., Husi, H., Yu, L., Brandon, J. M., Anderson, C. N., Blackstock, W. P., Choudhary, J. S., and Grant, S. G. (2006) *J. Neurochem.* **97,** S16–S23
68. Higgins, D. G., Thompson, J. D., and Gibson, T. J. (1996) *Methods Enzymol.* **266,** 383–402